



**Molecular probes for selective detection of cysteine  
cathepsins**

Journal:	<i>Organic &amp; Biomolecular Chemistry</i>
Manuscript ID	OB-REV-02-2021-000225.R1
Article Type:	Review Article
Date Submitted by the Author:	17-Mar-2021
Complete List of Authors:	Schleyer, Kelton A; University of Florida, Medicinal Chemistry Cui, Lina; University of Florida, Medicinal Chemistry

## ARTICLE

## Molecular probes for selective detection of cysteine cathepsins

Kelton A. Schleyer and Lina Cui\*

Received 00th January 20xx,  
Accepted 00th January 20xx

DOI: 10.1039/x0xx00000x

Cysteine cathepsins are proteases critical in physiopathological processes and show potential as targets or biomarkers for diseases and medical conditions. The 11 members of the cathepsin family are redundant in some cases but remarkably independent of others, demanding the development of both pan-cathepsin targeting tools as well as probes that are selective for specific cathepsins with little off-target activity. This review addresses the diverse design strategies that have been employed to accomplish this tailored selectivity among cysteine cathepsin targets and the imaging modalities incorporated. The power of these diverse tools is contextualized by briefly highlighting the nature of a few prominent cysteine cathepsins, their involvement in select diseases, and the application of cathepsin imaging probes in research spanning basic biochemical studies to clinical applications.

### Introduction

Cysteine cathepsins (CT's) are critical players in many physiological and pathological processes.<sup>1</sup> Typically restricted to the lysosomes, cathepsins degrade proteins for recycling, and their activity is also used to activate other enzymes, degrade cellular and structural biomacromolecules and contribute to inflammatory phenotypes. Cathepsin activity has also been detected in the nucleus,<sup>2, 3</sup> at the cell membrane,<sup>4</sup> and extracellularly,<sup>5</sup> reflecting its broad utility in a variety of cellular contexts.<sup>6</sup> The need for detection and imaging of cathepsins is important because cathepsins show promise as biomarkers for disease diagnosis<sup>7</sup> as well as suitable targets for *in vivo* imaging of cancer,<sup>8, 9</sup> atherosclerosis,<sup>10</sup> osteoporosis,<sup>11</sup> and other diseases.<sup>12</sup> In many cases, such as in clinical detection of tumours,<sup>13</sup> the simultaneous activity of multiple cathepsins and their overlapping substrate preferences<sup>14, 15</sup> makes imaging of cumulative activity appropriate.<sup>16</sup> However, each cysteine cathepsin does have distinct roles in physiology and pathology,<sup>12</sup> meaning that an accurate full-picture description of cathepsin activity must address each cathepsin selectively even in the presence of similar competing family members.<sup>13</sup> Depending on the disease state being studied and the type of experiment or clinical technique being performed, an imaging probe with desired characteristics is indispensable. In this review, we describe the considerations applied to designing molecular probes for a subset of coordinated cysteine cathepsins, including both probes that are selective for one or more targets and those that are pan-reactive to capture cumulative activity of cathepsins. We briefly introduce the role of cathepsins in physiology and diseases, then describe the

cathepsin-targeted imaging probes that have been designed, arranged by mechanism of signal contrast strategy. We highlight each design component that influences a probe's selectivity profile and describe the general trends reported in work. We close by describing the applications of these probes from bench to bedside, showing how the nature of the probe can provide specific desired information in the lab or clinic – or, rather, how different research and medical goals have inspired the development of this toolkit. The scope of this review is restricted to cathepsins B (CTB), K (CTK), L (CTL), S (CTS), V (CTV), and X (CTX), due to their overlapping nature in many aspects. Cathepsin activity and probe types are tabulated well in other reviews.<sup>17, 18</sup>

### Cathepsins in living systems

#### Tissue localization

Cathepsins exhibit distinct tissue distribution.<sup>7, 19–21</sup> At the tissue level, CTB and CTL are ubiquitously expressed, while CTK, CTS, and CTV have more restricted distribution. CTK expression is normally restricted to osteoclasts.<sup>22</sup> CTS exhibits specific tissue distribution in the spleen and heart and in lung macrophages, implicating an immune-related role.<sup>23</sup> CTV is relegated to the thymus and testes,<sup>20</sup> although high expression has been detected in certain malignant cell lines.<sup>19</sup>

#### Cellular localization

Cathepsins are most abundantly localized in lysosomes and related cellular structures, where they degrade proteins including internalized cell-surface and extracellular macromolecules. Some activities of nucleus-localized cathepsins<sup>2</sup> have also been described and are significant in some contexts.<sup>2, 24</sup> Altered cellular localization of cathepsins appears commonplace among different pathologies, although this aberrant trafficking and secretion may be influenced by different pathways for each cathepsin or for different cell

<sup>a</sup> Department of Medicinal Chemistry, College of Pharmacy, University of Florida, 1345 Center Dr, Gainesville, FL 32610

\* Correspondence should be addressed to linacui@cop.ufl.edu.

Electronic Supplementary Information (ESI) available: [details of any supplementary information available should be included here]. See DOI: 10.1039/x0xx00000x

types.<sup>9</sup> For instance, within tumour cells, increased cathepsin expression levels coupled with compromised mannose-6-phosphate-based protein trafficking results in flux of cathepsins to the extracellular space.<sup>7, 25</sup> Also in malignant cells, lysosomal CTB undergoes increased secretion, indicating higher excretion and extracellular activity of this cathepsin in the tumour microenvironment.<sup>26</sup> The acidic pH in the tumour microenvironment (due in part to increased metabolism) keeps extracellular cathepsins active, resulting in continued proteolytic activity. This altered cathepsin distribution can be influenced by extracellular factors. For example, in the tumour microenvironment, tumour-associated macrophages (TAMs) can excrete cathepsins resulting in extracellular activity and uptake of cathepsins by nearby tumour cells.<sup>27</sup>

### Biochemical functions

At the biochemical level, the most common cathepsin activity is lysosomal degradation of proteins, including internalized extracellular components, such as collagen.<sup>9</sup> Their major contributions occur through their enzymatic activity, so activity detection is the most reliable measure of their influence in biochemical processes. Cathepsins are tightly regulated, both translationally and post-translationally, at the mRNA and protein levels, and are expressed as pro-enzymes lacking enzymatic activity.<sup>28</sup> Even after activation by self (at low pH) or another enzyme, cathepsin enzymatic activity is strictly modulated by potent endogenous inhibitors such as cystatins, stefins, and serpins.<sup>18</sup> Because of this tight regulation at all levels, quantifying cathepsins at the mRNA or protein levels does not reliably correlate with enzymatic activity and can thus obfuscate results, although one example of a correlation between cathepsin mRNA expression level and relative activity level has been noted.<sup>29</sup> For instance, one study showed that atherosclerotic plaques exhibit diffuse CTK expression (based on immunofluorescence) but only a spatially restricted subset of this population was enzymatically active (determined using a quenched polymeric fluorescent probe, described later).<sup>10</sup> This experimental distinction was crucial in determining the localization and origin of enzymatically active CTK in this model. Cathepsin activity has been described as overlapping in some biological processes,<sup>1</sup> but certainly not all. Their substrate specificities also overlap significantly, making selective probing challenging.<sup>14</sup> This overlap is better resolved for naturally folded protein substrates, which tend to provide higher selectivity than small peptide strands.<sup>30</sup>

### Physiopathological contributions

Cathepsin enzymatic activity is involved in cell growth, migration, and signaling, and this activity is modified in many pathological contexts.<sup>7, 9, 12, 25, 31</sup> Members among the cysteine cathepsins demonstrate pathological activities that are concomitant but not exactly overlapping.<sup>32</sup> For instance, CTB, CTL, and CTS all contribute to atherosclerosis, but each through a different mechanism.<sup>33, 34</sup> In some contexts, one cathepsin can have an effect opposite to that of other cathepsins. For example, most cancers exhibit overexpression of CTL during the process of cell migration; however, the opposite was observed

in one HPV-driven cancer model, in which CTL deficiency was tumourigenic and its overexpression was protective against cancer progression.<sup>35-37</sup> Thus, sometimes probing for a single cathepsin is critical to determine desired information about a disease state, which may be obscured if multiple cathepsins are assayed using pan-cathepsin probes. Cathepsins show promise as biomarkers for cancers<sup>38-41</sup> and other diseases,<sup>42-45</sup> making detection of their activity either selectively or collectively, attractive.

**Cancers.** Upregulation of cathepsins has been observed both in cancer cells and in cancer-associated stromal cells, such as macrophages and fibroblasts.<sup>9, 46</sup> Cathepsins are implicated in almost every stage of tumour progression, including tumourigenesis, proliferation, invasion, angiogenesis, and metastasis.<sup>9</sup> Their contributions to cancer biology are, broadly, two-fold: cathepsins degrade extracellular matrix components or cell adhesion molecules, contributing to cell mobility, matrix remodeling, and downstream signaling, while also activating other pro-enzymes that have downstream tumourigenic effects.<sup>5, 9</sup> These two basic roles of cathepsins in cancer are made acutely influential by the aberrant and upregulated expression of cathepsins and increased levels of their secretion into the extracellular space.<sup>9</sup> Cathepsins are involved in cross-talk between different cell types in the tumour environment, with each cell type presenting a different cathepsin profile and influencing other cell types nearby to alter their cathepsin expression profiles.<sup>9, 47</sup> These cell type-specific and cathepsin-specific processes demand highly specific probes that can parse the role of a single cathepsin and track its generation from a particular cell type into the cancer microenvironment. The involvement of cysteine cathepsins in cancer is extensive and is thoroughly reviewed elsewhere.<sup>9, 25</sup>

**Cardiovascular diseases.** Many cardiovascular diseases are the result of extensive ECM remodeling in the walls of blood vessels. Atherosclerosis (the buildup of fats in artery walls) generates plaques comprised of fats, cholesterol, and various local and recruited cells, including leukocytes and macrophages.<sup>48</sup> As the plaque swells, smooth muscle cells generate ECM components to form and strengthen the fibrous cap that reinforces the inner vessel wall to prevent rupture. Unfortunately, recruited macrophages and other cells within the plaque increase the expression of ECM-degrading proteases like matrix metalloproteinases (MMPs) and cathepsins, which proceed to erode the fibrous cap, leading to plaque rupture.<sup>48</sup> The ECM-degrading activity of cathepsins also contributes to aortic aneurysms and to the process of restenosis<sup>49</sup> (a narrowed blood vessel that was medically cleared, but begins narrowing once again).<sup>50</sup> Cathepsins also influence other processes in the development of cardiovascular disease, such as uptake and storage of cholesterol and low-density lipoprotein.<sup>51, 52</sup> The myriad influence of cathepsin activity in atherosclerosis and other cardiovascular diseases has been reviewed previously.<sup>49, 53</sup> Of note, some cathepsins are potential biomarkers for cardiovascular diseases: both CTL and CTS serum levels correlate with coronary artery stenosis<sup>54, 55</sup> while CTS levels in serum may also be predictive of atherosclerotic development.<sup>56</sup>

**Other pathologies.** Osteoporosis is the gradual loss of bone density due to imbalances in the natural cycle of bone decomposition and reconstruction.<sup>57</sup> Osteoclasts are bone cells responsible for bone resorption, which they accomplish by binding to target bone structures and excreting hydrochloric acid and CTX,<sup>57</sup> a cathepsin boasting high collagenolytic proficiency.<sup>58</sup> As collagen is a major component of bone, the collagenolytic activity of CTX is clearly compatible with the excessive bone resorption that characterizes osteoporosis. In normal physiological conditions, osteoclasts are the only cells in the body that secrete detectably high levels of CTX,<sup>22</sup> giving potential for CTX-targeted imaging of related processes. Cathepsins are associated with inflammation and the breakdown of connective tissues that occurs in arthritis. CTX, along with CTB, CTL, and CTS is associated with arthritis,<sup>5</sup> but CTL and CTS serum levels do not correlate with disease severity, precluding their use as biomarkers except in seropositive patients.<sup>5</sup> Overall, cathepsins are linked to many diseases that involve inflammatory processes, in which cathepsins exert their

roles through enzymatic function, operating distinctively yet in a coordinated fashion depending on the context.<sup>59</sup>

## Design strategies of cathepsin probes

Imaging probes can be characterized by their typical mechanism of action, notably by (i) how they are recognized and/or activated by the target enzyme, (ii) how they generate signal contrast, and (iii) how they are tailored to improve these characteristics by interacting with the target enzyme, the environment, or the experimental system. Due to the significance of design to the possible applications of a probe, here we describe probes for the six selected cysteine cathepsins organized by design strategy. We highlight the principle of the strategy, the design features that influence selectivity and sensitivity, and provide examples of both pan- and selective cathepsin probes in each class. Although optical imaging has limited tissue penetration,<sup>60</sup> <sup>61</sup> most modern probe development starts with fluorescence-based detection due to

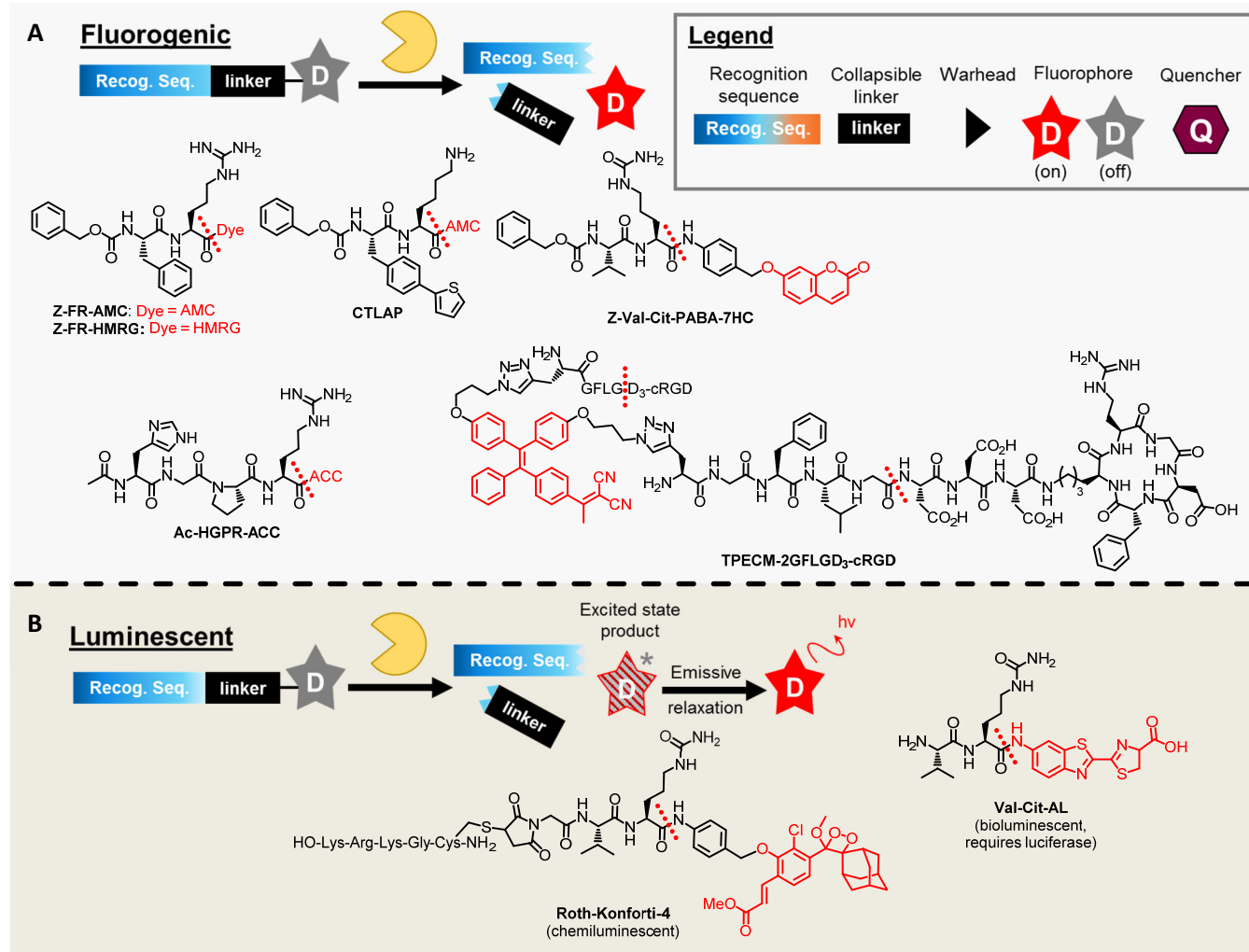


**Fig. 1** Design and structures of (A) fluorogenic and (B) chemiluminescent cathepsin probes. Probe components are listed in the legend. Reporters are shown in red, fluorescence quenchers in purple, and other detection/purification tags in green (for chemical structures, see Supplementary Chart 1). The colour spectrum used for the recognition sequence (blue to orange) reflects the changing amino acid preferences that occur across the cathepsin binding pocket, with blue depicting interactions with the N-terminal (unprimed) region of the binding pocket and orange depicting interactions with the C-terminal (primed) region of the binding pocket (see ref. 102). Red solid lines indicate the cathepsin enzymatic cleavage site(s) in each probe.

its high sensitivity, multiple detection wavelengths, and convenience of use via various laser-based instrumentations. Fluorescence-based detection has become the most common method for assaying and detecting cathepsin enzymatic activity *in vitro*, and optical imaging is a promising strategy for clinical diagnosis and has also found a niche in imaging-guided surgery.<sup>62-64</sup> Imaging with modalities other than fluorescence then follows.<sup>60</sup> This review also uses the following two terms for probe description: "substrate-based probes" refer in general to probes that require enzyme cleavage or activation of the substrate; these probes are typically named in accordance with their mechanism of signal generation, such as fluorogenic<sup>65</sup> or Förster resonance energy transfer (FRET)<sup>66</sup> probes. "Activity-based probes" (ABPs) are termed by the original publications because of their derivation from activity-based protein profiling, and they refer to probes that form covalent bonds at the catalytic site upon enzyme activation.<sup>67</sup> With few exceptions, all probes mentioned by name in this review are further described in Table 1, and their structures are provided in Figs. 1, 3, 4, and 5. The structures of common fluorophores, quenchers, and other chemical groups are provided in Supplementary Chart 1.

### Fluorogenic probes

Fluorogenic probes (Fig. 1A, Table 1) consist of a fluorophore covalently linked to a recognition sequence that elicits activity from the target enzyme. This covalent linkage masks the fluorescent emission<sup>68, 69</sup> of the reporter, but cleavage of this linkage by cathepsins restores high fluorescence emission through a mechanism called intramolecular charge transfer (ICT).<sup>70, 71</sup> This linkage is usually formed with a heteroatom (N, O) in the conjugated system of the fluorophore, preventing resonance and suppressing emission until the bond is broken. Common fluorogenic probes employ coumarin or xanthene dyes (such as fluorescein and rhodamine) as such a bond is easily formed; such an arrangement is not easily formed using

cyanine and BODIPY dyes, which are instead found in other types of probes.<sup>65</sup> Efficient cleavage of the covalent bond and the resulting increase in fluorescence quantum yield determines the sensitivity of the probe. Coumarin and xanthene dyes in cathepsin probes have reported varying turn-on ratios between dozens- to hundreds-fold.<sup>72-74</sup> The emission wavelength of the fluorophore is an important parameter to determine the suitability of a probe for a given application. For experiments in biological environments, the fluorophore emission wavelength must be detectable with minimal background interference from the environment; blue-wavelength coumarins are not ideal for cell-level experiments due to high cellular autofluorescence in this range,<sup>75</sup> so higher-wavelength reporters have been used in these contexts.<sup>76, 77</sup> The CTB-selective probe **Z-FR-HMRG** (Fig. 1A) used hydroxymethylrhodamine green (HMRG) as the reporter, enabling fluorescence imaging of cathepsins in cells and via colonoscopy in a mouse model (Fig. 2).<sup>73</sup> Another CTB-selective probe (**Wang-1**) used luciferin as its fluorescent reporter moiety and was targeted to the lysosomes by the addition of a lysosomotropic morpholine group, further improving its sensitivity by localizing the fluorescent signal to this organelle.<sup>78</sup>

Considering their suitability for probing cathepsins, aminocoumarins were the earliest fluorophores used in fluorogenic cathepsin probes, with 7-amino-4-methylcoumarin (AMC) and 7-amino-4-trifluoromethylcoumarin (AFC) being the most common.<sup>79-81</sup> A small yet significant chemical modification provided 7-amino-4-carbamoylmethylcoumarin (ACC), which was developed to make solid-phase synthesis of fluorogenic probes more accessible when creating large substrate screening libraries.<sup>82</sup> ACC also demonstrated a larger increase in quantum yield upon uncaging compared to AMC, without altering kinetics against the target protease.<sup>83</sup> This is significant as the structure of the chosen fluorophore can often affect the kinetics and selectivity profile of a probe.<sup>81</sup>

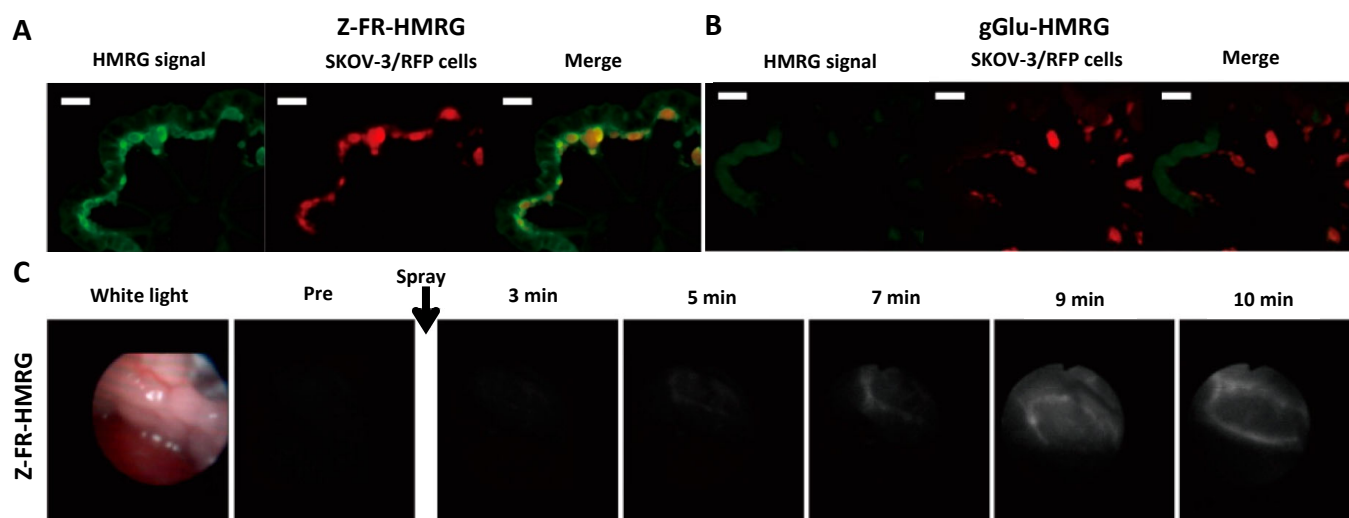


**Fig. 2** Visualization of ovarian tumour dissemination *ex vivo* and via endoscopy using cathepsin-targeting fluorogenic probes. (A,B) SK-OV-3/RFP (red signal) cells disseminated in the mesentery, stained with fluorogenic probe (green) for (A) cathepsins using **Z-FR-HMRG** or (B)  $\gamma$ -glutamyltransferase using **gGlu-HMRG**. Scale bars represent 5.0 mm. (C) *In vivo* endoscopy imaging of mouse abdominal cavity after spray application of **Z-FR-HMRG**. White light, image before probe application; fluorescence channel (grey scale), images after probe application. Adapted from Ref. 73 with permission. Copyright (2014) American Chemical Society.

The fluorophore can also be selected to accomplish both imaging and therapy purposes, termed ‘theranostics.’ In these systems, a released dye can generate both near-infrared fluorescence (NIRF) emission for imaging and singlet oxygen generation for photodynamic therapy (PDT), depending on the excitation wavelength used.<sup>84</sup> Such a PDT probe was developed using aggregation-induced emission reporters, in which a probe bears a hydrophobic aromatic reporter that can freely rotate and is therefore non-emissive.<sup>85</sup> Upon liberation from the probe by enzyme activity, the poorly soluble aromatic reporters aggregate, restricting their rotational freedom and greatly enhancing their emission intensity. This system was used to create a CTB probe (**TPECM - 2GFLGD<sub>3</sub> - cRGD**, Fig. 1A) that was applied to imaging and PDT *in vitro* in cancer cells.<sup>86</sup> Recognition of the pan-cathepsin sequence (Phe-Leu-Gly) by CTB released the tetraphenylethylene (TPE) AIE-gen that provided both fluorescence emission for imaging and singlet oxygen generation for photosensitization of cancer cells.<sup>86</sup>

Aggregation of nanoparticles can also provide cathepsin-responsive imaging and phototherapy. A cyanobenzothiazole-based “click” reaction<sup>87</sup> used CTB activity to cross-link chlorin-e6 (Ce6)-labeled upconversion nanocrystals (cathepsin-responsive upconversion nanocrystal, **CRUN**, Table 1, structure not shown).<sup>88</sup> The *in situ* bundling of **CRUN** in response to CTB activity was used for *in vivo* tumour imaging and PDT in mice.<sup>88</sup>

Photophysical or photochemical processes other than fluorescence can be harnessed to elicit photon emission in response to cathepsin activity. A chemiluminescent probe (Fig. 1B) for CTB boasted remarkably high sensitivity for CTB detection (**Roth-Konforti-4**, Fig. 1B).<sup>89</sup> The probe caged Schaap’s adamantylidene-dioxetane reporter<sup>90</sup> using a CTB recognition sequence; CTB activity released the phenolate-dioxetane reporter which spontaneously decomposed to form an excited-state benzoate ester which subsequently relaxed by emission of a 470 nm photon, generating readout signal. This probe demonstrated exquisite sensitivity for detecting CTB, with a limit of detection (LOD) of 1.75 pM, while the comparator fluorogenic probe **Z-Val-Cit-PABA-7HC** (Fig. 1A) gave an LOD of 28.73 nM, a 16,000-fold difference in sensitivity.<sup>89</sup> A luciferin-based bioluminescence probe for CTB, **Val-Cit-AL** (Fig. 1B), was also created in which cathepsin activity unmasked a luciferin functional group that could then undergo oxidative decarboxylation upon reaction with the luciferase enzyme.<sup>91</sup> This luciferin-luciferase reaction generated 560 nm emission upon relaxation of the excited-state product, serving as the readout signal for CTB activity.

While the fluorophore provides the signal of the probe, the recognition sequence of a probe is an extended chemical structure that is recognized by the cathepsin active site and accommodates enzymatic turnover of the probe. Natural cathepsin substrates are peptides, and cathepsin activity is driven primarily by the structures of only two or three amino acids in the substrate sequence.<sup>14, 30</sup> Thus, simple di- or tri-peptide probes bearing coumarin fluorophores (e.g., **Z-FR-AMC**) served as the first-generation fluorogenic probes for characterizing cathepsins<sup>19, 81, 92-95</sup> and assaying their activity in

pathology and physiology studies.<sup>26, 96</sup> Cysteine cathepsins exhibit overlap in substrate specificity,<sup>14</sup> so these probes could be activated by multiple cathepsins or members of other enzyme classes. While not entirely selective, these simple probes can still exhibit one- to dozens-fold selectivity (in terms of relative  $k_{cat}/K_M$  values) for one cathepsin.<sup>14, 97, 98</sup> Combinatorial chemistry screening libraries and methods were developed to synthesize sequences of all possible amino acid combinations, identifying more selective recognition sequences by taking full advantage of minor differences in cathepsin substrate preferences. From these efforts, probes bearing exclusively natural amino acids were created which demonstrated excellent efficiency and up to 100-fold selectivity even among cysteine cathepsins (e.g., **Ac-HGPR-ACC**, Fig. 1A).<sup>14, 30</sup> Including non-natural amino acids in these libraries further distinguished cathepsin preferences and provided probes with selectivity factors in the thousands.<sup>28, 98, 99</sup> While extensive, such combinatorial libraries are limited by the amino acids they contain<sup>14, 98, 99</sup> and should consider the possibility that cooperativity between substrate residues may not be detected using some combinatorial methods.<sup>99</sup>

‘Perfect’ selectivity among enzymes is ideal for molecular probes and therapeutic agents,<sup>13</sup> and new methods, such as innovative approaches for library generation, are needed to generate cathepsin probes with even greater selectivity. Although cathepsins overlap in recognizing primary amino acid sequences, they do show greater selectivity in recognizing the tertiary structure of natural substrates.<sup>18</sup> Thus, libraries of cyclic peptides (such as those generated using phage display<sup>100</sup>) and other recognition sequences bearing higher-order structure may provide probes with greater selectivity for a single cathepsin.<sup>101</sup>

To generate fluorogenic probes, a fluorophore needs to be attached to the enzyme substrate via an amide bond that is cleavable by the catalytic machinery of the enzyme (Fig. 1). Therefore, cathepsin substrate specificity is achieved predominantly by substrate binding to the N-terminal side of the catalytic site, called the ‘unprimed’ region according to Schechter and Berger nomenclature.<sup>102</sup> This leaves the fluorophore as the only portion of the probe in proximity to the C-terminal (‘primed’) region of the binding pocket, precluding access to these residues to create further binding recognition and improve turnover efficiency and selectivity.<sup>103, 104</sup> As smaller fluorogenic probes often lack strong selectivity, experimental protocols for their use in biological samples have included steps that deactivate competing enzymes, such as the addition of an inhibitor selective for undesired cathepsins<sup>34, 38, 43, 105</sup> or pre-incubating the samples under harsh conditions.<sup>106</sup> Introduction of unnatural functional groups to peptide side chain can not only affect the binding selectivity to specific cathepsins,<sup>107</sup> but also improve the detection efficiency of the probe.<sup>72</sup> Via introducing a dual-quenching mechanism, the Cui lab developed a dipeptidyl-AMC probe, **CTLAP** (Fig. 1A), which demonstrated improved selectivity for CTL over CTB (15-fold) and even CTV (7-fold) that can potentially preclude these preparative steps.<sup>72</sup> The recognition sequence of the probe

TABLE 1. Notable molecular imaging probes for cathepsins

Probe ID	Design principle	Imaging modality (reporter)	Selectivity	Applications	Refs.
Ac-HGPR-ACC	Fluorogenic	Fluorescence (350/450 nm)	CTK >> CTB,L,S,V	<i>In vitro</i>	14
CTLAP	Fluorogenic	Fluorescence (380/450 nm)	CTL > CTB,V >> CTS	<i>In vitro</i>	108
TPECM-2GFLGD <sub>3</sub> -cRGD	Fluorogenic (AIE)	Fluorescence (405/560 nm)	CTB (selectivity n.d.)	<i>In vitro</i>	86
Wang-1	Fluorogenic	Fluorescence (350/525 nm)	CTB >CTD,L,S	<i>In vitro</i>	109
Z-FR-AMC	Fluorogenic	Fluorescence (380/450 nm)	CTL > CTB,V >> CTS	<i>In vitro</i>	34
Z-FR-HMRG	Fluorogenic	Fluorescence (497/521 nm)	CTB >> CTL	<i>In vitro, in vivo, ex vivo</i>	110
Z-Val-Cit-PABA-7HC	Fluorogenic	Fluorescence (360/455 nm)	CTB (selectivity n.d.)	<i>In vitro</i>	89
Roth-Konforti-4	Chemiluminescent	Chemiluminescent (n.a./470 nm)	CTB (selectivity n.d.) <sup>111</sup>	<i>In vitro</i>	89
Val-Cit-AL	Bioluminescent	Bioluminescence (luciferase/590 nm)	CTB (selectivity n.d.) <sup>111</sup>	<i>In vitro, in vivo</i>	91
6QC 6QC-NIR 6QC-ICG	FRET	Fluorescence (6QC: 640/670 nm) (6QC-NIR: 710/820 nm) (6QC-ICG: 805/835 nm)	CTL > CTV >> CTB,K,S	<i>In vitro, in vivo</i>	16, 112-118
AW-091	FRET	Fluorescence (710/780 nm)	CTS >> CTB,K,L	<i>In vitro, in vivo</i>	119
CRUN	FRET (nanoparticle)	Fluorescence (640/670 nm) Phototherapy (808 nm)	CTB (selectivity n.d.)	<i>In vivo, ex vivo</i>	88
CyA-P-CyB	FRET	Fluorescence (635/755 nm) Phototherapy (808 nm)	CTB (selectivity n.d.) <sup>120, 121</sup>	<i>In vivo</i>	122
DEATH-CAT-2 DEATH-CAT-FNIR	FRET	Fluorescence (DEATH-CAT-2: 640/670 nm) (DEATH-CAT-FNIR: 765/788 nm)	CTL >> CTB,S	<i>In vitro, in vivo</i>	118
FAP-CAT	FRET	Fluorescence (640/670 nm)	CTL >> CTB,S	<i>In vitro, in vivo</i>	118
FFCD 1	FRET	Fluorescence (480/515 nm)	CTB (selectivity n.d.)	<i>In vitro</i>	123
Hu-3	FRET	Fluorescence (680/700 nm)	CTS > CTB,CTK,CTL,CTV	<i>In vitro, in vivo</i>	124
Legowska-1	FRET	Fluorescence (320/420 nm)	CTL	<i>In vitro</i>	125
LUM015	FRET	Fluorescence (650/675 nm)	CTS, trypsin > CTK,L >> CTB	<i>In vivo, ex vivo</i>	126-129
MG101	FRET (hairpin loop)	Fluorescence (680/703 nm)	CTS > CTL >> CTB,K	<i>In vitro</i>	130
Pc-FcQ	FRET	Fluorescence (622/708 nm)	CTB (selectivity n.d.)	<i>In vitro, in vivo</i>	131
Tholen-5	FRET	Fluorescence (640/670 nm)	CTB,CTS > CTL	<i>In vitro, in vivo, ex vivo</i>	16
Tholen-6	FRET	Fluorescence (640/670 nm)	CTB,CTS > CTL	<i>In vitro</i>	16
Watzke-2	FRET	Fluorescence (336/468 nm)	CTK >> CTB,L,S	<i>In vitro</i>	132
Watzke-4	FRET	Fluorescence (336/468 nm)	CTS > CTL >> CTB,K	<i>In vitro</i>	132
Watzke-5	FRET	Fluorescence (544/573 nm)	CTL > CTS >> CTB,K	<i>In vitro</i>	132
CPGC	FRET (polymer)	Fluorescence (673/689 nm)	CTB (selectivity n.d.)	<i>In vivo</i>	133, 134
L-SR15	FRET (polymer)	Fluorescence (680/715 nm) Phototherapy (650 nm)	CTB > CTL,S	<i>In vivo, ex vivo</i>	135, 136
ProSense680	FRET (polymer)	Fluorescence (650/700 nm)	CTD (selectivity n.d.)	<i>In vitro, in vivo</i>	137
Sensor I	FRET (polymer)	Fluor. lifetime (750/800 nm)	CTL,S, plasmin, elastase, trypsin >> CTB,K	<i>In vitro</i>	138
Hingorani-1	CEST MRI	MRI ( $\delta = 5.2, 9.5$ ppm)	CTS (selectivity n.d.)	<i>In vitro</i>	139
PLG	CEST MRI (polymer)	MRI (water, $\delta = 0$ ppm)	CTB (selectivity n.d.)	<i>In vivo</i>	140
GB111	ABP	Fluorescence (532/580 nm)	CTB,L > CTS,X	<i>In vitro, in vivo</i>	141
GB123	ABP	Fluorescence (633/680 nm)	CTB,L	<i>In vitro, in vivo, ex vivo</i>	33, 142, 143
GB138	ABP	Fluorescence (780/820 nm)	CTB,L	<i>In vitro, in vivo</i>	142
Huisman-7	ABP	Fluorescence (405/500+ nm)	CTL > CTB,S	<i>In vitro</i>	144
Huisman-8	ABP	Fluorescence (450/650 nm)	CTL,S >> CTB	<i>In vitro</i>	144
MP-cB-1	ABP	Fluorescence (633/670 nm)	CTB >> CTL,S > CTK,V	<i>In vitro</i>	98
MP-cB-2	ABP	Fluorescence (633/670 nm)	CTB >> CTK,L,S,V	<i>In vitro, ex vivo</i>	98
MP-cB-3	ABP	Fluorescence (750/780 nm)	CTB >> CTK,L,S,V	<i>In vitro</i>	98
MP-cl3	ABP	Fluorescence (633/670 nm)	CTL > CTB,V >> CTK,S	<i>In vitro</i>	99
MP-pc1	ABP	Fluorescence (633/670 nm)	CTB,S > CTK,L,V	<i>In vitro</i>	99
MP-pc3	ABP	Fluorescence (550/570 nm)	CTB,S > CTK,L,V	<i>In vitro</i>	99
sCy5-Nle-SY	ABP	Fluorescence (633/670 nm)	CTX > CTS >> CTB,L	<i>In vitro</i>	145

TCpABP	ABP	Fluorescence (488/505 nm)	CTB,F,H,L,O,S,Z	<i>In vitro</i>	29
Torkar-1	ABP (Photoaffinity)	Cross-linking (365 nm) Fluorescence (532/580 nm)	CTL > CTV >> CTB,K	<i>In vitro</i>	146
<sup>68</sup> Ga-BMV101 ( <sup>64</sup> Cu-BMV101)	ABP	PET ( <sup>68</sup> Ga); Fluorescence (633/670 nm) PET ( <sup>64</sup> Cu); Fluorescence (633/670 nm)	CTB > CTS > CTL,X	<i>In vivo</i>	147, 148
<sup>64</sup> Cu-GB170	ABP	PET ( <sup>64</sup> Cu); Fluorescence (633/670 nm)	CTB,L	<i>In vivo</i>	149
<sup>90</sup> Y-BMX2	ABP	PET ( <sup>90</sup> Y); Fluorescence (n.r.)	<i>Not reported,</i>	<i>In vitro, in vivo</i>	150
BMV083	qABP	Fluorescence (633/670 nm)	CTS > CTB,L	<i>In vitro, In vivo, ex vivo</i>	151
BMV109	qABP	Fluorescence (633/670 nm)	CTB,L,S,X	<i>In vitro, In vivo, ex vivo</i>	46, 152, 153
BMV157	qABP	Fluorescence (633/670 nm)	CTS > CTB >> CTL,X	<i>In vitro, in vivo, ex vivo</i>	154
GB117	qABP	Fluorescence (532/580 nm)	CTL > CTB > CTS,X	<i>In vitro, in vivo</i>	141
GB137	qABP	Fluorescence (633/680 nm)	CTL > CTB >> CTS,X	<i>In vitro, in vivo, ex vivo</i>	142
LES13	qABP	Fluorescence (650/670 nm) Fluorescence (pH) (420/520 nm)	CTL,S > CTB,X	<i>In vitro</i>	155
VGT-309	qABP	Fluorescence (745/820 nm)	CTB,L > CTX >> CTS	<i>In vitro, in vivo</i>	156
YBN08	qABP	Fluorescence (710/760 nm) Phototherapy (654 nm)	CTB,L,S	<i>In vitro</i>	157
YBN14	qABP	Fluorescence (710/760 nm) Phototherapy (760 nm)	CTB,L,S	<i>In vitro, in vivo</i>	157, 158
DARPin 8h6	Binding-based	Fluorescence (675/720 nm)	CTB >> CTK,L,S,X	<i>In vitro, in vivo, ex vivo</i>	59

contained a 2-phenylthiophene moiety which improved selectivity for CTL (in accordance with previous findings<sup>107</sup>) while also quenching the background emission of the AMC reporter, resulting in over 100-fold turn-on ratio from the probe.<sup>108</sup>

The fluorophore and recognition sequence may be connected via a chemical linker or spacer. These spacers are typically 'sacrificial' or 'self-immolative' and they decompose upon response to the target enzyme, resulting in traceless release of the recognition sequence and the fluorophore.<sup>159</sup> The structure of the linker can influence probe kinetics<sup>160</sup> and improve selectivity by influencing the steric interactions between the probe and the enzyme active site.<sup>97</sup> A notable example is the inclusion of a para-aminobenzaldehyde (PABA) linker, which tends to increase the selectivity of probes for CTB over CTL, even in small dipeptidyl-AMC probes.<sup>97</sup> The linker can also affect other properties pertinent to biological applications, such as serum stability or biodistribution.<sup>159</sup>

Fluorogenic probes have strengths and weaknesses compared to other classes of probes. Introduction of different fluorescence quenching mechanisms to fluorogenic probes can sometimes provide higher efficiency than FRET probes.<sup>66, 161</sup> In addition, unlike ABPs (described later), most of the fluorogenic cathepsin probes do not covalently label their target enzyme.<sup>46</sup> Future probe design with features for *in situ* labeling can potentially further improve the efficiency of the fluorogenic cathepsin probes.

### FRET probes

Conjugating a donor fluorophore and an acceptor fluorophore, the absorption of which overlaps with the donor's emission,<sup>162</sup> in close proximity (< 10 nm) can result in a reduced fluorescence emission of the donor, due to Förster resonance energy transfer (FRET, Fig. 3).<sup>17, 66</sup> When the donor and acceptor are linked through an enzyme substrate, upon the substrate cleavage, the two fluorophores diffuse apart and the emission of the donor is

restored. This strategy has been widely used to detect the activity of a range of enzymes, including cathepsins.<sup>17</sup> Different mechanisms and strategies of FRET are possible and have been reviewed elsewhere.<sup>66</sup>

Many standard FRET dye-quencher pairs have been established and applied to cathepsin probes, ranging from blue-wavelength FRET pairs like 2-aminobenzoyl (Abz) and 2,4-dinitrophenol (Dnp) to dyes in the NIR range.<sup>112, 163</sup> This expansive wavelength range enables the use of FRET probes even in complex *in vivo* applications. In a CTB-responsive FRET probe/photosensitizer, **Pc-FcQ** (Fig. 3A), photosensitizing zinc (II) phthalocyanine dye was quenched by a ferrocenyl BODIPY that was conjugated through a CTB-selective substrate (Gly-Phe-Leu-Gly-Lys).<sup>131</sup> In another work, a pan-CT FRET probe used a two-photon dye (DL-1) as the reporter, enabling the use of low-energy excitation wavelengths (750-860 nm).<sup>164</sup> The fluorescent signal of FRET probes can also be masked by something other than a small molecule organic acceptor dye. A quenched graphene oxide-based nanoprobe was developed for CTB-selective detection, in which the graphene oxide itself served as the quencher for the Ce6 emitter/photosensitizer.<sup>165</sup>

FRET-based quenching can produce significant signal turn-on ratios, with the simple donor/acceptor pair Abz/Dnp exhibiting between 7- to 100-fold emission increase upon substrate hydrolysis.<sup>166</sup> A CTB-responsive probe with the NIR pair Cy5.5/BHQ-3 displayed a remarkable 50-fold turn-on ratio *in vitro*.<sup>163</sup> Concerns have been echoed about structural impediments of the dye/quencher pair selected for FRET probes, such as intact donor/acceptor pairs undergoing intramolecular stacking and self-quenching, or the nonspecific affinity of charged dyes to the negatively charged polynucleotides or cellular membranes.<sup>17</sup> Such issues should be examined and addressed as part of the characterization of a new probe.

Different from the fluorogenic probes, the recognition sequence of FRET probes can span both the 'primed' and

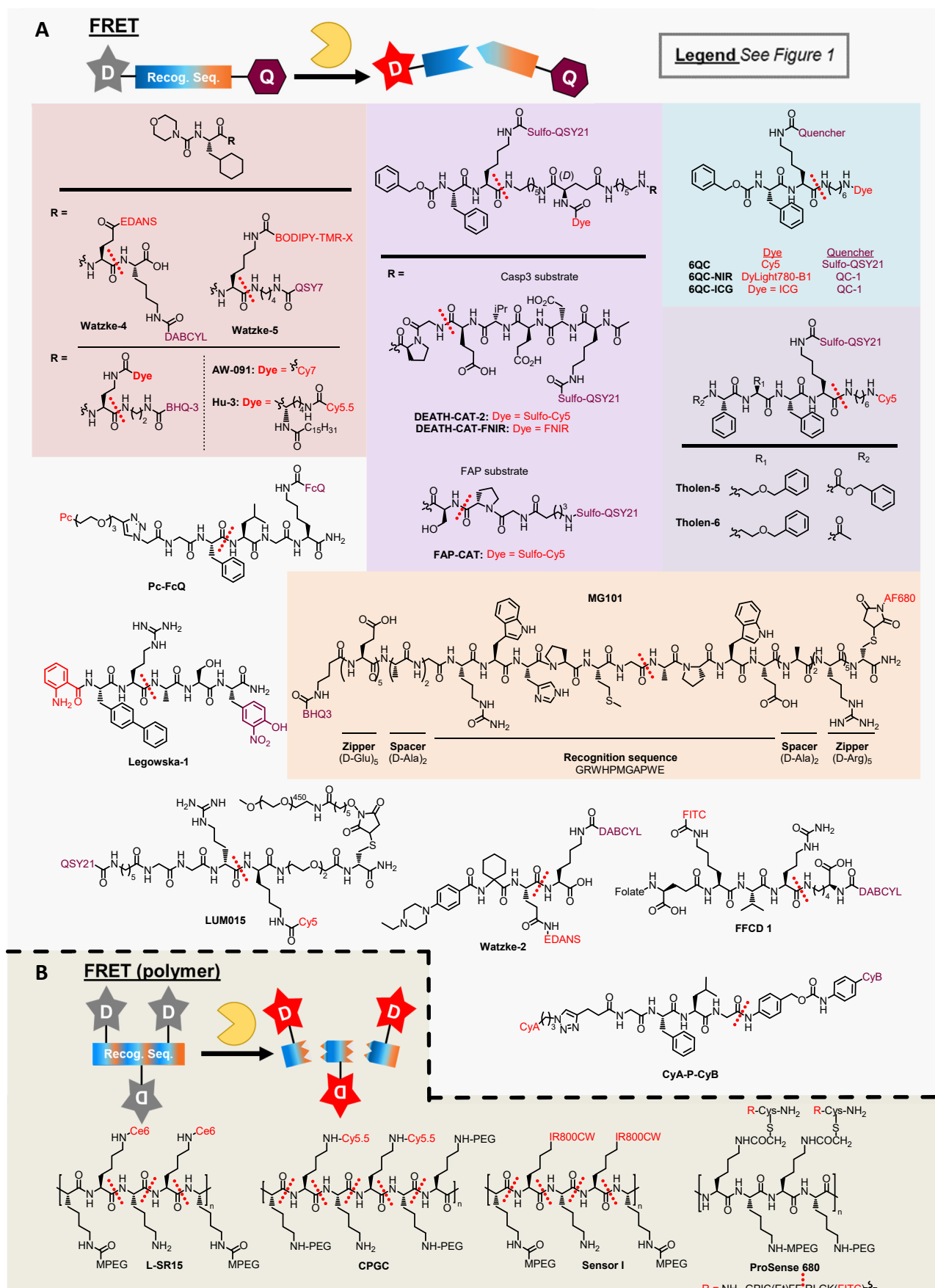


Fig. 3 Mechanism and structures of (A) FRET and (B) FRET polymer probes for cysteine cathepsin activity. For explanation of legend and color-coding, see Fig. 1.

'unprimed' regions of the enzyme active site.<sup>102</sup> Initial FRET probes for cathepsins used simple di- to pentapeptides labeled with donor/acceptor pairs like DANSYL/pNP or DANSYL/Dnp; these simple recognition sequences provided approximately 10-fold selectivity among cysteine cathepsins.<sup>167, 168</sup> While small dipeptidyl recognition sequences have facilitated excellent FRET probes for cathepsins,<sup>16, 112</sup> longer substrate sequences can more often result in greater turnover efficiency and selectivity due to increased interacting groups.<sup>18</sup> This was exemplified by the creation of a highly CTL-selective FRET probe (**Legowska-1**, Fig. 3A) which screened amino acids on both the 'primed' and 'unprimed' regions of the cathepsin L active site.<sup>125</sup> This probe could detect CTL activity in melanoma cell lysate with a limit of detection of 9.67 pM.<sup>125</sup> In this probe, 2-aminobenzoic acid (Abz) served as the donor and 3-nitrotyrosine served as the acceptor. FRET probes using longer peptide sequences have also been designed for CTB,<sup>169</sup> CTS,<sup>170</sup> and CTK.<sup>103, 104</sup> This strategy of utilizing both sides of the binding pocket can overcome other structural phenomena as is observed in the fluorogenic probes, such as steric collision of the fluorophore with active site residues which is common in CTB due to the presence of an occluding loop near the enzyme active site.<sup>169</sup> One FRET probe brought a dye/quencher pair together using a hairpin loop motif bearing a selective CTS substrate sequence (**MG101**, Fig. 3A).<sup>130</sup> Changing the dye and quencher to different molecules and swapping their location on either end of the loop altered the potency ( $k_{\text{cat}}/K_{\text{M}}$  for CTS reduced by half) but improved selectivity for CTS over other cathepsins. Complete selectivity for CTS against CTL was achieved by increasing the assay pH to 7.4, just outside the active pH range of CTL<sup>130</sup> (a strategy also used to remove off-target CTL activity by the CTB probe **Z-FR-HMRG**<sup>73</sup>). As demonstrated with **CTLAP**, non-canonical peptide sequences can also provide selectivity,<sup>108</sup> such as a cross-linked di-tyrosine sequence used in a CTB-selective probe.<sup>171</sup> This probe exhibited minimal cross-reactivity with CTL, however the blue wavelengths of its reporter limit its applications.<sup>171</sup>

Highly selective FRET probes have also been developed using the structures of selective peptide inhibitors as the recognition sequence. This strategy, known as 'reverse-design,' was used in the development of three selective probes for CTK or CTS.<sup>132</sup> The CTK-selective probe (**Watzke-2**, Fig. 3A) is based on a selective CTK inhibitor showing thousand-fold selectivity over CTB and CTS (based on  $IC_{50}$ ).<sup>172</sup> The probe used the dye/quencher pair EDANS/DABCYL (Supplementary chart 1) and showed 10-fold selectivity for CTK over CTL and 20-fold selectivity over CTB, while CTS was unresponsive to the probe. Likewise, the two CTS-selective probes (**Watzke-4** and **Watzke-5**, Fig. 3A)<sup>132</sup> were designed from a selective CTS inhibitor.<sup>173</sup> **Watzke-4** showed two-fold selectivity for CTS over CTL (negligible response to CTK, CTB, or papain), while changing the dye/quencher pair to BODIPY TMR-X/QSY-7 and attaching them to longer alkyl chains in the **Watzke-5** probe reversed the selectivity to two-fold in favor of CTL over CTS. This can be attributed to the drastic change in fluorophore size from EDANS to BODIPY TMR-X and the change of the P1 residue in the

recognition sequence from Glu to Lys, which is preferred by CTL.<sup>99</sup>

The N-terminal capping group of the recognition sequence can be selected to influence probe reactivity, solubility, and cell permeability. For instance, a small peptide FRET probe (**Tholen-6**, Fig. 3A) capped by an acyl group showed 9-fold greater response to cathepsins in cell lysate compared to an analogue capped by a carboxybenzyl group (Cbz); however, the Cbz-capped probe (**Tholen-5**, Fig. 3A) exhibited greater cell permeability and labeled whole cells with 3-fold greater intensity than the acyl-capped probe.<sup>16</sup>

While FRET systems usually involve a heterotypic pair of dye and quencher molecules, quenching can also occur between two similar fluorophore molecules, known as homo-FRET.<sup>162</sup> This phenomenon is also distance-dependent and occurs when identical fluorophores are bundled together in close proximity (~10 nm).<sup>174</sup> This phenomenon is leveraged by polymer-based FRET probes, which are polymers of repeating recognition sequences heavily labeled with dye molecules (Fig. 3B).<sup>133, 134, 175</sup> The close proximity between the dyes quenches 95-99% of their fluorescence, which is restored as cathepsin activity releases the individual dyes.<sup>133, 134</sup> One of the first polymer probes, **CPGC** (Fig. 3B), was a synthetic graft copolymer comprised of poly-L-lysine, a recognition sequence for CTB.<sup>133, 134</sup> The lysine side chains were capped with either methoxy poly(ethylene glycol) (MPEG) or Cy5.5 dyes, with the remainder being left exposed to elicit cathepsin activity upon recognition of the Lys-Lys motif (average labeling ratio 92 MPEG; 11 Cy5.5; 44 unlabeled). The resulting **CPGC** (approx. 490 kDa in mass and 100 nm in linear length) exhibited 15-fold reduced fluorescence compared to free Cy5.5, and processing by cathepsins restored 95% of the quenched fluorescence (giving a 12-fold turn-on ratio).<sup>134</sup> Similarly, a polymer-based FRET probe was used to visualize CTK activity in atherosclerosis.<sup>10</sup> It demonstrated about 2-fold selectivity for CTK over CTB and CTL and 14-fold selectivity against MMP-2/9 *in vitro* and exhibited a 9-fold turn-on ratio. A poly-Glu-based polymer FRET probe bearing NIR813 dyes exhibited selectivity for CTL and CTB over other proteases, based on mutual recognition of glutamine.<sup>176</sup> A similar polymer-based strategy was also brought to nanoparticle scaffold.<sup>177</sup>

While de-quenching of bundled fluorophores restores fluorescence intensity, it also restores the emission lifetime of the liberated fluorophores from a rapid decay (when quenched) to a normative (slower) decay upon liberation. The polymer FRET probe **Sensor I** (Fig. 3B) was used to detect cathepsin activity by measuring the emission lifetime of the released fluorophores instead of the emission intensity.<sup>138</sup>

Standard FRET probes have also been equipped for theranostics. A FRET probe using two Cy7 derivatives as dye and quencher (**CyA-P-CyB**, Fig. 3A) was developed to image CTB activity via NIR signal (635 nm excitation, 755 nm emission) and to execute PDT at 808 nm excitation.<sup>122</sup> The selectivity of this probe against other cathepsins was not tested but the substrate sequence (Gly-Phe-Leu-Gly) has been used for CTB-responsive prodrugs.<sup>120, 121</sup> Theranostic FRET polymer platforms have also been created for cathepsins using Ce6 as the reporter/photosensitizer.<sup>135</sup>

Like all probes, FRET probes can be functionalized to improve other characteristics, such as cell uptake or tumour targeting. Incorporation of a lipid group improved the cellular uptake of the CTS-selective FRET probe **Hu-3** (Fig. 3A), enabling live cell imaging.<sup>124</sup> FRET probes can also be targeted to cellular compartments or specific receptors to improve probe retention or localization.<sup>178</sup> For instance, a CTB-selective FRET probe was functionalized with folic acid, localizing the resulting fluorescent signal to cell-surface folate receptors.<sup>123</sup> This FITC-based probe (**FFCD 1**, Fig. 3A) generated a 10-fold turn-on ratio *in vitro* and a 4- to 7-fold turn-on ratio in cells based on flow cytometry. This folate receptor-targeting strategy is also found in other FRET cathepsin probes.<sup>165</sup> A pan-cathepsin FRET probe (**6QC**, Fig. 3A) used a lysosomotropic group to localize a liberated dye in the lysosomes of tumours in mice.<sup>112</sup> When equipped with the NIR dye indocyanine green (ICG), the resulting probe **6QC-ICG** (Fig. 3A) provided great sensitivity during imaging-guided surgery as the surgical instrumentation cameras were optimized for the FDA-approved ICG reporter.<sup>113</sup>

To improve tumour-selective imaging, a series of AND-gated FRET probes were developed.<sup>118</sup> These probes contained two quenchers, each linked to a central dye by a recognition sequence for a different cancer-associated protease with increased expression compared to normal tissues (e.g. cathepsins and caspase-3<sup>179</sup>). The AND-gated probes (**DEATH-CAT-2**, **DEATH-CAT-FNIR**, and **FAP-CAT**, Fig. 3A) exhibited higher tumour-to-background fluorescence ratios than probes responding to only one protease, validating the AND-gate design. Another recent study created a screening library of cathepsin probes whose activities were assayed directly in tumour cell extracts instead of with purified cathepsins in buffer.<sup>16</sup> This *in situ* screening selected probes that were suited for this environment (**Tholen-5** and **Tholen-6**), avoiding the need to validate candidate probes in a second experimental step. This direct target-based screening can provide probes pre-tailored to respond to a selected disease state.

#### Substrate-based probes using other imaging modalities

Chemical exchange saturation transfer (CEST) magnetic resonance imaging (MRI) probes activated by cathepsins have been designed.<sup>139, 140</sup> These probes contain functional groups (such as amides or carboxylic acids) bearing exchangeable protons which can be selectively saturated by MR and subsequently transferred to nearby water molecules, leading to greatly altered bulk water signal (Fig. 4).<sup>180</sup> Modifications to the functional groups of these probes by cathepsin activity either enhances or attenuates this CEST signal, giving cathepsin-induced contrast.<sup>180</sup> One poly-glutamate probe (**PLG**, Fig. 4) was used to image a 9L rat brain gliosarcoma model, however the low sensitivity of the probe required injection of 160 mg/kg probe in rats.<sup>140</sup> A similar CEST MRI probe (**Hingorani-1**, Fig. 4), was developed to detect CTB activity; the probe used ratiometric analysis of the saturation signals from the aryl amide and the carboxylic acid moieties of the 4-amino-2-hydroxybenzoic acid released by CTB.<sup>139</sup> These MRI probes require no reporters such as fluorophores, heavy metals, or radiolabels while retaining the high tissue penetration of MRI

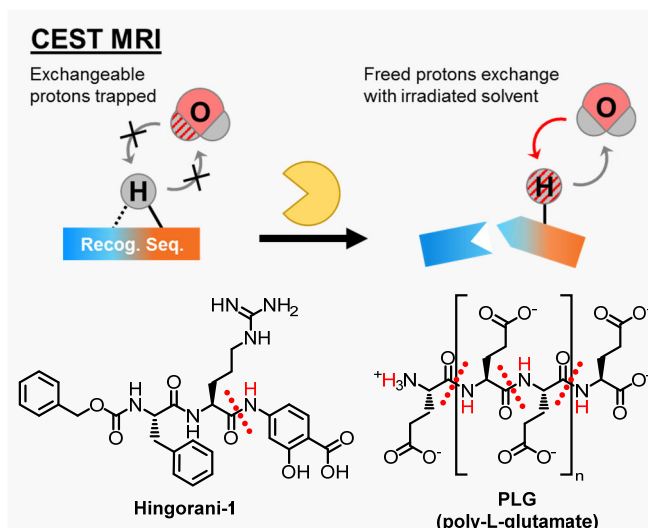


**Fig. 4** Mechanism and structures of CEST MRI probes for cathepsin activity. Exchangeable protons are labelled in red, and cleaved bonds are depicted in thick red lines.

and enhanced sensitivity caused by modifying the bulk water signal; they provide a complementary toolkit for translation to clinical molecular imaging.<sup>139</sup> More cathepsin-activated MRI agents are reviewed elsewhere.<sup>180</sup>

#### Activity-based probes (ABPs)

##### Design and Mechanism

Activity-based probes (ABPs) are extended from the proteomic technique known as activity-based protein profiling (ABPP).<sup>181</sup> To sample only active proteins within a complex mixture (such as living cells or tissue lysate), these techniques created probes that could covalently label active enzymes.<sup>182</sup> The resulting ABPs could be labeled with affinity, fluorescence, or radiolabel tags for purification and characterization of the tagged enzymes.<sup>181, 183</sup> ABPs are designed to contain a labeling tag, a linker, and a warhead, the latter defined as a chemical group that can establish a covalent bond with the enzyme catalytic machinery upon enzymatic activation (Fig. 5). The warhead is typically electrophilic in nature and can covalently link with the nucleophilic catalytic residue. The warhead is designed to have only moderate reactivity that is directed by the selectivity of the recognition sequence.<sup>181</sup> Interestingly, the warhead can sometimes favor response to different protease classes.<sup>18, 184, 185</sup> Some common warheads used in cathepsin-targeting ABPs include epoxide,<sup>29, 144</sup> azanitrile,<sup>186</sup> and vinyl sulfone<sup>187, 188</sup> groups. Selectivity for cysteine cathepsins over other mechanistic classes of proteases can also be achieved using the acyloxymethyl ketone (AOMK) warhead (see Fig. 5B),<sup>189</sup> which has enjoyed wide use among recent cathepsin ABPs.<sup>141, 142</sup> The more electron-deficient 2,3,5,6-tetrafluoro-phenoxy methyl ketone (PMK) group shows higher overall reactivity and thus ABPs with this warhead tend to label more cysteine cathepsins than they would otherwise.<sup>152</sup> For example, use of the AOMK warhead on a particular scaffold resulted in some selectivity for CTB and CTL (**GB137**, Fig. 5B),<sup>142</sup> while conversion to the PMK warhead resulted in broader labeling of CTB, CTL, CTS, and CTX

(BMV109, Fig. 5B).<sup>152</sup> This was attributed both to the increased reactivity of the PMK group as well as its dec

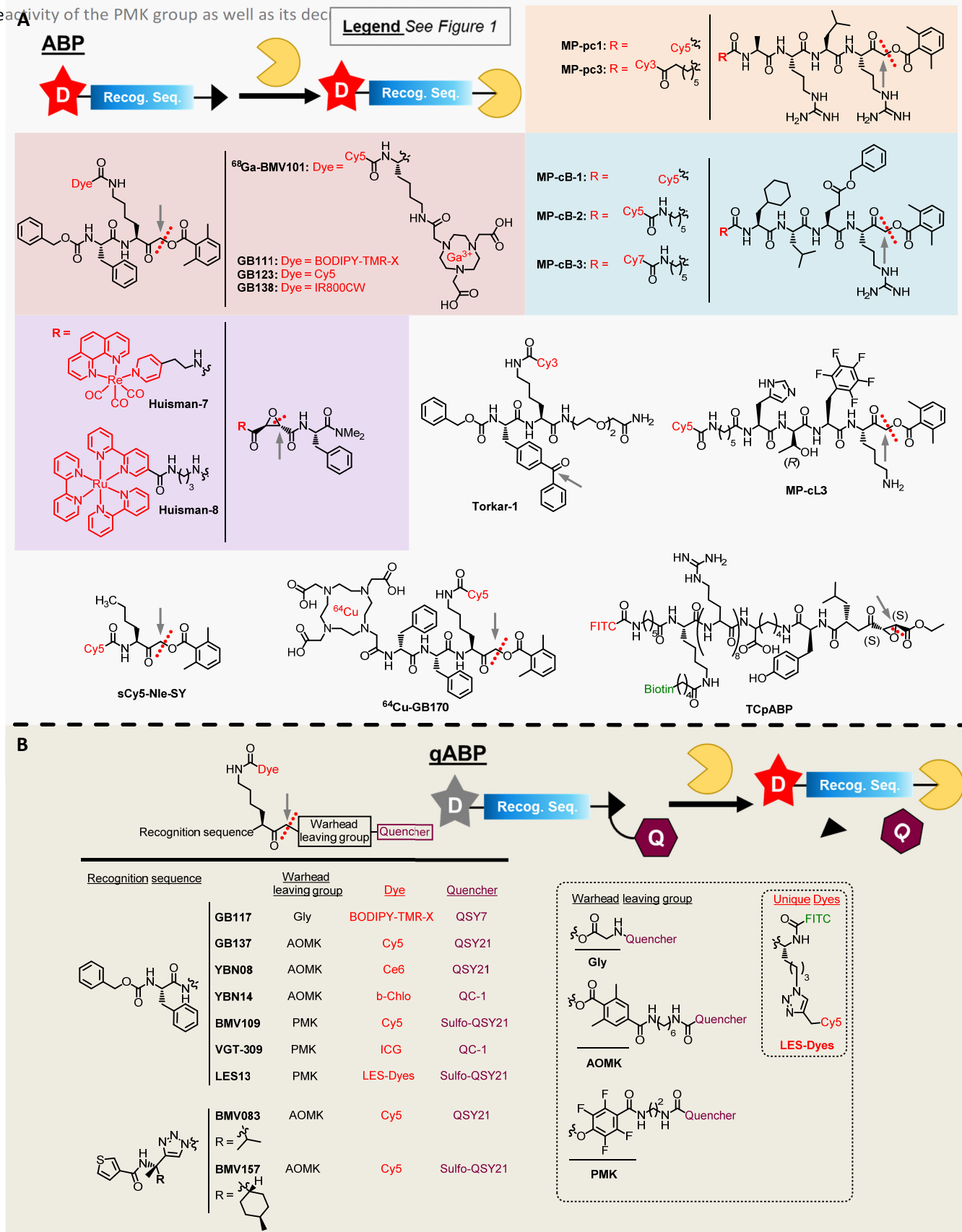


**Fig.5** Mechanism and structures of unquenched (A) and quenched (B) activity-based probes for cysteine cathepsin activity. Red groups depict reporter moieties, while green groups are alternative tags for detection or isolation. For explanation of legend and color-coding, see Fig. 1. The site of covalent linkage is shown with a gray arrow.

steric bulk, which likely collided with the cathepsin binding sites.<sup>152</sup>

In ABPs, probe selectivity is mainly contributed by the recognition sequence. Short, pan-cathepsin sequences provide broad-spectrum ABPs useful for overall activity quantification (**BMV109**).<sup>141, 142, 152</sup> Selective sequences derived from library screening or reverse-design have provided highly selective ABPs for CTL (**MP-cl3**, Fig. 5A)<sup>99</sup> and CTB (**MP-cb-2**)<sup>98</sup> or CTS (**BMV157**, Fig. 5B),<sup>152, 154</sup> respectively. Boasting both high selectivity and high sensitivity, these probes are attractive candidates for clinical and translational applications.

The location and structure of the fluorophore can influence probe selectivity and potency. Swapping the N-terminal biotin group of **MP-cl2** (not shown) for a Cy5 fluorophore increased the potency of the resulting **MP-cl3** for CTL by 10-fold ( $k_{obs}/I$ ), indicating that reporter selection can influence kinetics even when located far away from the cathepsin active site.<sup>99</sup> Increasing the size of the N-terminal reporter of the CTB probe with balanced efficiency and selectivity. It is also noted that due to their irreversible inhibition of the target enzyme, ABPs tend to exhibit lower selectivity at later time points compared to substrate-based probes that do not label, as inhibition of the target enzyme increases the potential for off-target labeling by remaining ABP after long periods of time.<sup>98</sup> Probe components can also influence its performance *in vivo*. Inclusion of sulfate groups on the dye and quencher can improve probe solubility, changing the required injection dose and biodistribution.<sup>18, 154</sup> For example, changing the Cy5 reporter of **GB123** (Fig. 5A) to an 800CW reporter (**GB138**, Fig. 5A) altered the biodistribution of the probe in a mouse tumour model, resulting in improved tumour labeling and reduced off-target labeling in the liver, spleen, and kidneys.<sup>142</sup> Sequential-labeling techniques (administration of ABP, followed by labeling with a dye) have been used when inclusion of a dye reduced probe affinity for the target protease.<sup>190</sup>

The linker included between the reporter and the recognition sequence may also affect potency at the desired target<sup>112</sup> as well as other probe characteristics. In one series of ABPs, a simple glycine linker between the AOMK warhead and the quencher was unstable against serum esterases, while a bulkier aminobutyric acid (AIB) linker improved stability; an extended hexamethylenediamine linker greatly improved serum stability while also increasing CTB activity (by displacing N-terminal quencher from CTB occluding loop thus reducing steric repulsion).<sup>142</sup> In the development of CTL-selective probe **MP-cl3**, inclusion of a 6-ahx linker between the N-terminal cyanine reporter and the peptide sequence reduced potency for CTL by 3-fold but increased selectivity to some extent against all competing cathepsins by 1- to 8-fold (**MP-pc1** vs. **MP-pc3**, Fig. 5A).<sup>99</sup> These trends were also observed in pan-cathepsin probes with nonspecific recognition sequences, supporting the hypothesis that the structures of these probe components have direct influence on the activity and selectivity profiles of the probes against their target(s). These effects were echoed in a subsequent study developing ABPs selective for CTB: inclusion of an ahx linker retained potency against CTB while increasing

selectivity against CTL and CTS, the best competing cathepsins in this work (**MP-cb-1** vs. **MP-cb-2**, Fig. 5A).<sup>98</sup>

ABPs may contain a fluorophore that is always emissive (termed 'unquenched ABPs', see Fig. 5A) or may contain a dye/quencher pair as in FRET probes (termed 'quenched ABPs' or 'qABPs', see Fig. 5B). However, unless a fluorescence quenching group is present in the unreacted probe, *in situ* resolution of the active probe requires removal of unreacted probe molecules from the experimental system, either by washing in cell-based experiments<sup>98, 99, 144</sup> or by blood circulation *in vivo*.<sup>142</sup>

### Unquenched ABPs

Original cysteine cathepsin ABPs were unquenched, having an always-on fluorescent signal and accomplishing contrast exclusively by covalent labeling of the target enzyme.<sup>185</sup> This requires removal of unbound probes using washing steps for cell-based experiments<sup>99</sup> or product isolation/purification such as SDS-PAGE of protein mixtures or cell lysates;<sup>144</sup> *in vivo* analyses may require several hours for probe clearance to establish optimal tumour-to-background signals for unquenched probes.<sup>142</sup>

Simple azadipeptide nitrile ABPs have been developed, with some analogues exhibiting pan-cathepsin (CTB, CTL, CTK, CTS) activity and others having more selective profiles (e.g. 10-fold selectivity for CTK over CTS with little response from CTB and CTL).<sup>186</sup> Pan-cathepsin ABPs were preliminary developments but, depending on applications, are still powerful tools that are useful alone or in combination with other labeling tools.<sup>141, 142</sup> Pan-reactive ABPs have improved diagnostic tools for conditions involving multiple macrophage-generated cathepsins.<sup>191</sup> In most cases these probes favor CTB and CTL in terms of labeling potency but other targets (CTS, CTK) are also labeled to a detectable extent. An unquenched coumarin-tetrahydroquinoline-labeled vinyl sulfone peptide ABP was 3-fold and 60-fold more selective ( $k_{inact}/K_i$ ) for CTS over CTL and CTB/CTK, respectively;<sup>188</sup> this selectivity for CTS is attributed to interactions between the S3 subsite of CTS and the fluorophore.<sup>188, 192</sup> Thus, the fluorophore structure can also influence the selectivity of the probe. Another vinyl sulfone-based ABP was equipped with an irreversibly locked GFP-like fluorophore; it was pan-reactive but had most selectivity for CTS and preferred CTS and CTK over CTL and CTB.<sup>187</sup>

One CTL-selective photoaffinity-based ABP, **Torkar-1**, was developed by equipping the recognition sequence with a reversible amide warhead and a photoreactive benzophenone moiety (Fig. 5A).<sup>146</sup> Under normal conditions, the amide warhead reversibly binds with CTL, but irradiation with 365 nm light results in covalent cross-linking of the benzophenone with nearby residues in the CTL binding pocket and achieving target labelling.<sup>193</sup> The location of the benzophenone cross-linking moiety significantly influenced selectivity of **Torkar-1** between CTL and CTB, with the final structure yielding approximately 4-fold selectivity for CTL over CTV and 20-fold selectivity over CTB, based on in-gel fluorescence results.<sup>146</sup>

A series of CTB-selective, AOMK-bearing ABPs were developed.<sup>194</sup> Activity of the original AOMK-warhead probe was

selective for CTB, but swapping the AOMK warhead for an epoxide also resulted in CTX labeling, attributed to reduced steric hindrance from the smaller epoxide group with the active site of CTX. This selectivity was compromised in samples other than cell lysates, but pre-incubation with an AOMK-based pan-cathepsin inhibitor enabled CTX-selective labeling in live cells and *ex vivo* samples.<sup>194</sup> Other groups achieved improved CTX selectivity by using a sulfoxonium ylide warhead, with the best probe **sCy5-Nle-SY** (Table 1, Fig. 5A) showing selective CTX detection in cell lysates and cells containing low CTS levels, and negligible labeling of CTB and CTL.<sup>145</sup> The probe enables selective labeling of CTX in SDS-PAGE; while cross-reactivity with CTS is observed in living macrophages and *in vivo* in mice, it is the most selective CTX probe reported to date.<sup>145</sup>

Transition metal-based luminophores have also been used to design ABPs for cysteine cathepsins. A line of Re(I) and Ru(II)-based luminescence probes were designed for CTL (**Huisman-7**, **Huisman-8**, Fig. 5A).<sup>144</sup> These probes contained an epoxide warhead and a recognition sequence based on the CTL-selective inhibitor CLIK-148;<sup>195, 196</sup> they covalently labeled CTL by the attack of the active-site cysteine to open the epoxide. The Re- and Ru-based emitters showed broad emission curves around 500-700 nm and notably long emission lifetimes (9.5  $\mu$ s for Re-based **Huisman-7**, and 0.9  $\mu$ s for Ru-based **Huisman-8**), making their signals distinct from those of cellular autofluorescence (fluorescence emission of biomolecules such as aromatic amino acids, nucleobases, and porphyrins, typically having emission lifetimes between 1-10 ns<sup>197</sup>). The potency and selectivity of the probes for CTL were altered greatly by installing the Re- and Ru-based reporter groups. Compared to its unlabeled counterpart, installation of the Re(phen)(CO)<sub>3</sub> reporter in **Huisman-7** increased its potency against CTL 16-fold by causing both tighter reversible binding and faster inactivation. The selectivity for CTL over CTS increased 5-fold, resulting in 222-fold selectivity against this competitor (CTB was inhibited poorly by **Huisman-7**).<sup>144</sup> Notably, the Ru(bpy)<sub>2</sub>-coordinated probe **Huisman-8** bearing an extended propyl spacer between reporter and recognition sequence, compromised the potency and selectivity of the parent inhibitor, decreasing the  $k_{\text{inact}}/K_i$  value by 5-fold and reducing the CTL/CTS selectivity to 1.5-fold.

Unquenched ABPs have been further functionalized to improve their characteristics. Installation of a poly-arginine cell-penetrating peptide (CPP) onto pan-cathepsin sequence bearing FITC and biotin tags gave a trifunctional cell-permeable activity-based probe (**TCpABP**, Fig. 5A) that improved cellular uptake for whole-cell labeling prior to lysis and proteomic analysis (see Applications section).<sup>29</sup>

#### Quenched ABPs

Quenched ABPs (qABPs) use FRET mechanisms to provide signal contrast while retaining their capacity to covalently label the target enzyme.<sup>178</sup> Thus, qABPs exhibit low fluorescence emission until activated by the target enzyme, resulting in contrast both from target labeling and from recovered fluorescence. Pan-cathepsin qABPs have been designed using a combination of broad-spectrum recognition sequences and the highly reactive PMK warhead, such as **BMV109** for labeling CTB,

CTL, CTS, and CTX.<sup>152</sup> Changing the dye/quencher pair of **BMV109** to ICG/QC-1 gave the pan-cathepsin probe **VGT-309** (Fig. 5B) for *in vivo* optical imaging.<sup>156</sup> Pan-cathepsin probes can be modified or altered to generate more selective probes. For example, the unquenched ABP **GB111** (Fig. 5A) labeled CTL and CTB with equal potency.<sup>141</sup> Simple addition of the quencher QSY7 to the C-terminal AOMK warhead gave the qABP **GB117** (Fig. 5B), which reduced affinity for both CTB and CTL but increased selectivity for CTL, likely because the quencher clashed sterically with the CTB occluding loop.<sup>141</sup> The pan-cathepsin qABP **GB137**<sup>142</sup> was modified to be highly CTS-selective by switching the recognition sequence to either of two CTS-selective inhibitor sequences, giving qABPs **BMV083** (Fig. 5B) and **BMV157**.<sup>151, 154</sup>

Cathepsin-targeted qABPs have also been developed for theranostics. The CTB/CTL-selective ABP **GB111** was equipped with a Ce6 dye/photosensitizer and the quencher QSY21 to create a photosensitizer-qABP (PS-qABP) theranostic cathepsin probe (**YBN08**, Fig. 5B).<sup>157</sup> Release of the quencher activated the Ce6 fluorophore and the photosensitizer. The quenched analogues of the probe exhibited 14- to 363-fold quenched signal compared to unquenched ABP analogues. **YBN08** probe labelled CTB, CTL, and CTS equipotently in intact macrophages and tumour cells and was also used for *in vivo* optical imaging and PDT in mice. Using other photosensitizer/quencher pairs (e.g., b-Chlo/QC-1), similar PS-qABPs were developed (**YBN14**, Fig. 5B).<sup>158</sup>

Cathepsin qABPs have also demonstrated dual-channel imaging capacity.<sup>155</sup> One qABP, **LES13**, was functionalized with a FITC moiety to sense pH changes; this enabled simultaneous detection of both cathepsin activities and pH changes in macrophages upon infection by *Salmonella typhimurium*.<sup>155</sup>

#### ABPs using other imaging modalities

Optical imaging is one of many imaging modalities used for *in vivo* medical imaging, which also includes positron emission tomography (PET), computed tomography (CT), and magnetic resonance imaging (MRI). We direct the readers to other reviews regarding the nature of these imaging methods and their strengths and weaknesses.<sup>60</sup> The spatial resolution provided by covalent labeling of ABPs makes them attractive platforms for imaging probes of any one modality or multi-modalities. For example, a dual-modality NIRF(Cy5)/PET(<sup>64</sup>Cu) probe (**<sup>64</sup>Cu-GB170**, Fig. 5A) was developed for PET imaging of solid tumors using <sup>64</sup>Cu for its positron emission and Cy5 for optical visualization in complementary assays.<sup>149</sup> Notably, the Cy5 fluorophore enhanced tumour uptake compared to the PET-only analog. ABPs for PET imaging of cathepsins have been reported, such as an <sup>18</sup>F-labeled nitrile cathepsin ABP.<sup>192</sup> The semi-CTB-selective PET probe **<sup>68</sup>Ga-BMV101** (Fig. 5A) was in clinical trials for patients with idiopathic pulmonary fibrosis (NCT02485886) between 2015 and 2017.<sup>198</sup>

Compared to other types of imaging probes, the primary strength of ABPs is the ability to covalently label their target enzyme. Conventional substrate-based probes suffer from signal diffusion while ABPs label the active enzyme and therefore remain at the site of activation.<sup>67, 199</sup> However, ABPs

block the enzyme active site and prevent further activity of the linked enzyme.<sup>185</sup> This single-cycle reactivity limits signal amplification, the advantage we can take while measuring enzymatic activities. Whether substrate-based probes or ABPs generate more signal is a topic of contention; strategies incorporating *in situ* labeling while maintaining the enzymatic activity for signal amplification are more desirable.

#### Binding-based probes

Binding-based (or affinity-based) probes bind with the enzyme reversibly and typically have a reporting moiety that is always active. Such binding-based probes have found applications in targeting cancer-associated ligands, such as the folate receptor, integrins, and prostate-associated membrane antigen in developing imaging probes or targeted prodrugs.<sup>178</sup>

One binding-based probe for CTB has been developed using a designed ankyrin repeating protein (DARPin) system. The probe, **8h6** (Table 1), demonstrated that selectivity could be achieved by targeting an allosteric (non-active-site) sequence, as cathepsin active sites are highly conserved.<sup>59</sup> This was corroborated by kinetic characterization of the **8h6**-CTB complex, which depicted a mixed inhibition mode that could still process substrate, albeit very slowly.<sup>59</sup> The probe boasted high affinity for CTB ( $K_i = 35$  pM) with no detectable binding to CTK, CTL, CTS, or CTX, revealing the high selectivity possible for binding-based probes. Both direct and secondary fluorescent antibodies are also commercially available for many cathepsins (via Santa Cruz Biotechnology, Invitrogen, Abcam); these are widely used to image and quantify total cathepsin protein expression levels in cells and tissue samples, sometimes in complement with probes for activity (Fig. 6).<sup>99</sup>

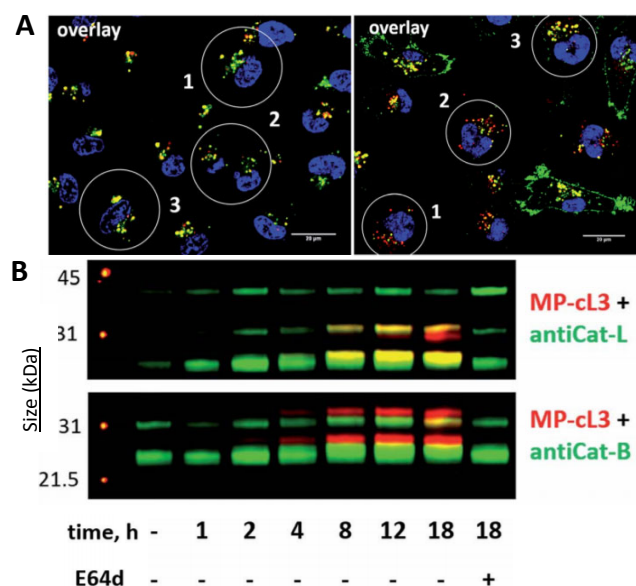


**Fig. 6** Selective detection of CTL activity in cancer cells using activity-based probe MP-cL3. MDA-MB-231 cells were incubated with MP-cL3 for 8 h, washed and fixed, labelled with anti-cathepsin antibodies, and imaged by fluorescence microscopy. (A) Overlay of CTL probe MP-cL3 with anti-CTL antibody (left) or anti-CTB antibody (right), in MDA-MB-231 cells. E64d is a pan-cathepsin inhibitor. (B) In-gel fluorescence of MP-cL3 (red) and CTL- or CTB-selective antibodies (green). Selectivity for CTL over CTB is retained during the first 8 h of labelling. Adapted from Ref. 99 with permission. Copyright (2018) Royal Society of Chemistry.

## Applications of cathepsin imaging probes

The design of cathepsin-targeting imaging probes allows for many applications from basic research to clinical settings, with some imaging agents even being in clinical trials. In this section we highlight the representative applications of cathepsin imaging probes both *in vitro* (including test tube or plate-based assays, gel-based experiments, cell-based imaging, and *ex vivo* applications) and *in vivo* (including imaging of both mice and humans), along with a brief description of probes in clinical trials and their outcomes if completed.

#### *In vitro*

Simple fluorogenic dipeptidyl probes are commonly used to assay activity of cathepsins in microplate-based drug screening or similar assays. They can also be used to quantify cathepsin activity in cell lysate, clinical sample homogenate, or in excretions of cultured live cells.<sup>26</sup> Several fluorogenic AMC- or AFC-based probes are available as commercial kits for CTB, CTK, CTL, CTS, and CTV, although they are not fully selective for the listed target.<sup>97, 105</sup>

For clinical samples, these fluorogenic cathepsin probes have been used to detect overall cathepsin activity, complementing measurements of expression levels. This has been a common technique for determining the usefulness of cathepsin activity as a biomarker for diseases. In cancer, CTB and CTL activities show promise as diagnostic biomarkers. CTB and CTL activity in breast,<sup>40</sup> gallbladder,<sup>38</sup> and colorectal<sup>41</sup> tumour lysates correlated with the histological grade of the tumour and poor prognosis overall. Notably, these studies used non-specific fluorogenic probes (**Z-FR-AMC**), requiring the addition of a selective inhibitor to distinguish the activity of CTB and CTL in the mixed samples.<sup>34, 38, 43, 105</sup> In pediatric acute myeloid leukemia, CTL activity in isolated peripheral blood mononuclear cells and bone marrow mononuclear cells showed strong, independent potential for prognosis in patients, and activity decreased during administration of chemotherapy.<sup>43</sup> Again, this study required parallel assay of a sample containing a selective CTB inhibitor to accurately determine CTL activity, theoretically doubling the quantity of patient samples required to run the analysis. These combinations of probe and inhibitors were used with resected mouse aortic smooth muscle and endothelial cell lysates to determine the specific contributions of CTL activity to atherosclerosis in mice.<sup>34</sup> A more recently developed CTL-selective FRET probe **Legowska-1** could detect CTL activity in melanoma cell lysate with a limit of detection of 9.67 pM,<sup>125</sup> showing the benefits of highly selective FRET probes.

Along with substrate-based probes, ABPs have been used for biomarker determination. The CTS-selective qABP **BMV083** predominantly labeled M2 macrophages in a 4T1 mouse mammary adenocarcinoma model, suggesting that CTS activity can potentially serve as a prognostic marker for (activated) M2 macrophage development;<sup>151</sup> this shows potential for using highly selective CTS probes for diagnostic purposes. These experiments revealed further CTS selectivity by using neutral pH, taking advantage of the retained activity of CTS at this pH compared to CTB and CTL.<sup>151</sup> The pan-cathepsin ABP **GB123** was

used to determine the potential of CTB and CTS as biomarkers of rheumatoid arthritis and osteoarthritis in serum and synovial fluid.<sup>143</sup> CTB activity in both fluids correlated with osteoarthritis severity, while CTS levels served as a suitable biomarker for conditions of synovitis and rheumatoid arthritis.<sup>143</sup> In fluids, probe incubation was followed by SDS-PAGE analysis to quantify specific response of CTB and CTS, as CTL was also labelled. This is one drawback, as *in situ* quantification was likely not accurate for each independent cathepsin. Regardless, both selective and pan-cathepsin probes can successfully capture the independent activity of multiple cathepsins to provide clinically useful information. **GB123** was also used to image CTB and CTS activity in the lysate of chondrocytes isolated from the knee cartilage of arthritis patients;<sup>143</sup> the results could guide the follow-up *in vivo* diagnosis of disease progression using MRI- or PET-compatible cathepsin probes, due to the presence of cathepsin activity in certain stages of this disease.

### Cell-based experiments

Cell-based imaging of cathepsin activity is well established with numerous examples.<sup>86, 152</sup> Cathepsins have unique cellular distribution, however in diseases cathepsins experience altered localization patterns<sup>9, 26</sup> and cathepsin profiles can be unique to specific cell types.<sup>9, 47</sup> Cathepsin probes have enabled visualization of cathepsin activity at the whole-cell and sub-cellular levels. A cresyl violet-based fluorogenic probe measured the activity of CTB, CTL, and CTS within cells in a mixed-cell sample. Immunofluorescence labeling for cell type identification was paired with cathepsin signal to create a flow cytometry assay for quantifying cathepsin activity in single cells even in heterogeneous cell populations.<sup>200</sup> In a cancer-related study, the CTS-selective qABP **BMV083** selectively labeled bone marrow-derived macrophages (BMM) co-cultured with mammary tumour cells (4T1) due to CTS expression being localized exclusively within BMM cells.<sup>151</sup> Going further, sub-cellular localization of CTS was accomplished using one CTS-selective (**BMV157**) and one pan-cathepsin qABP with complementary fluorescent reporters.<sup>154</sup> The cellular localization of CTS was compared to overall cathepsin distribution in BMMs, demonstrating the high resolution made possible using ABP cathepsin probes.<sup>154</sup> CTL and CTB localization and activity overlap extensively, but the use of CTL-selective ABP **MP-cl3** and fluorescent anti-CTB antibodies enabled researchers to distinguish altered localization of CTL and CTB among organelles (Fig. 3).<sup>99</sup> This distinction was made possible by the high selectivity of the CTL probe and was also demonstrated for the related CTB-selective probe **MP-cb-2**.<sup>98</sup>

Cell imaging and subsequent proteomic analysis can also be achieved using ABPs. Pan-cathepsin-targeted, biotin and FITC dual-labeled ABP **TCpABP** was developed for cathepsin profiling in living cells<sup>29</sup> and gel-based mass spectrometry analysis using a pan-cathepsin sequence.<sup>201-203</sup> The FITC reporter and CPP sequence enabled cellular localization studies using fluorescence microscopy, while the biotin tag enabled subsequent cell lysis, bead-based enrichment, and SDS-PAGE and LC-MS/MS analysis to quantify and identify a multitude of labelled cathepsins including CTO and CTF (which are not

typically observed).<sup>29</sup> However, in this particular example, 52 non-cathepsin proteins were also labelled, partially due to non-specific interactions with the CPP sequence.<sup>29</sup>

### *In vivo* tumour imaging

Selective or pan-cathepsin probes may find specific benefits in certain applications.<sup>13</sup> Cathepsin activity probes have been used for *in vivo* imaging of the following types of cancer models: mammary adenocarcinoma or breast cancer,<sup>59, 118, 124, 151, 154, 156, 157</sup> intraperitoneally planted ovarian tumours;<sup>73</sup> and intestinal and colorectal cancers.<sup>46, 112, 115, 152, 204</sup>

The first cysteine cathepsin probes for *in vivo* imaging were polymer FRET probes,<sup>205</sup> which are currently commercially available under the name 'ProSense' and have still found favor in recent experiments.<sup>204, 206-208</sup> These probes were originally applied to *in vivo* imaging of tumours implanted into the mammary fat pad,<sup>134</sup> brain,<sup>209</sup> ear,<sup>210</sup> breast orthotopically,<sup>211</sup> and others.<sup>212</sup> Several studies have helped method development for applications of polymer FRET probes to endoscopic imaging of intestinal and colon cancers.<sup>46, 213-215</sup> They are also commonly used as comparative controls for newly developed probes.<sup>127</sup>

Small molecule FRET probes have also been used widely for *in vivo* imaging.<sup>112, 113</sup> The FRET probe **6QC-NIR** (Table 1, Fig. 3A) was preclinically evaluated for use in colorectal cancer.<sup>112</sup> Recently, it was used for combined white-light and NIR fluorescence-guided endoscopy of colorectal cancer, detecting adenomas down to 2.0 mm in size in rats and maintaining a tumour-to-background ratio of approximately 1.81 even in the presence of high background tissue inflammation.<sup>115</sup> Such probe applications could enable targeted biopsy directed by endoscopy results, reducing the amount of biopsy tissues required of patients. Recent work applied AND-gated FRET probes to *in vivo* cancer imaging and imaging-guided surgery in mice.<sup>118</sup> The AND-gated probes, **DEATH-CAT-2** and **FAP-CAT**, were brighter than single-target probe **6QC** to image 4T1 breast tumours and could detect lung metastases less than 1 mm in diameter in mice (**DEATH-CAT-2** was brighter than **FAP-CAT** in this experiment). Due to aggregation of the ICG probe the reporter was switched to FNIR-Tag<sup>216</sup> (and the quencher was switched to QC-1) to give **DEATH-CAT-FNIR**, which could detect lung metastases in real time dissection using Firefly and LiCor Pearl imaging systems.<sup>118</sup>

Small molecule ABPs and qABPs have also progressed to *in vivo* cancer imaging. Fluorescent qABPs for cysteine cathepsins were debuted by the Bogyo lab<sup>141</sup> and subcutaneous tumour imaging was later demonstrated in mice.<sup>142</sup> Both pan-cathepsin and selective ABPs have successfully imaged tumours in mice. The pan-cathepsin qABP **BMV109** was used for *in vivo* imaging of breast cancer in mice and confirmed the involvement of cathepsins in CD68<sup>+</sup> tumour-associated macrophages (Fig. 7).<sup>152</sup> It has also been tested in preclinical models for imaging colorectal cancer.<sup>46</sup> The pan-cathepsin qABP **VGT-309** was used for *in vivo* imaging of 4T1 mouse mammary tumours implanted in the mouse flank, followed by imaging-guided surgery to remove the tumours.<sup>156</sup> Two qABP's currently boasting the highest selectivity for CTS within their class, **BMV083** and

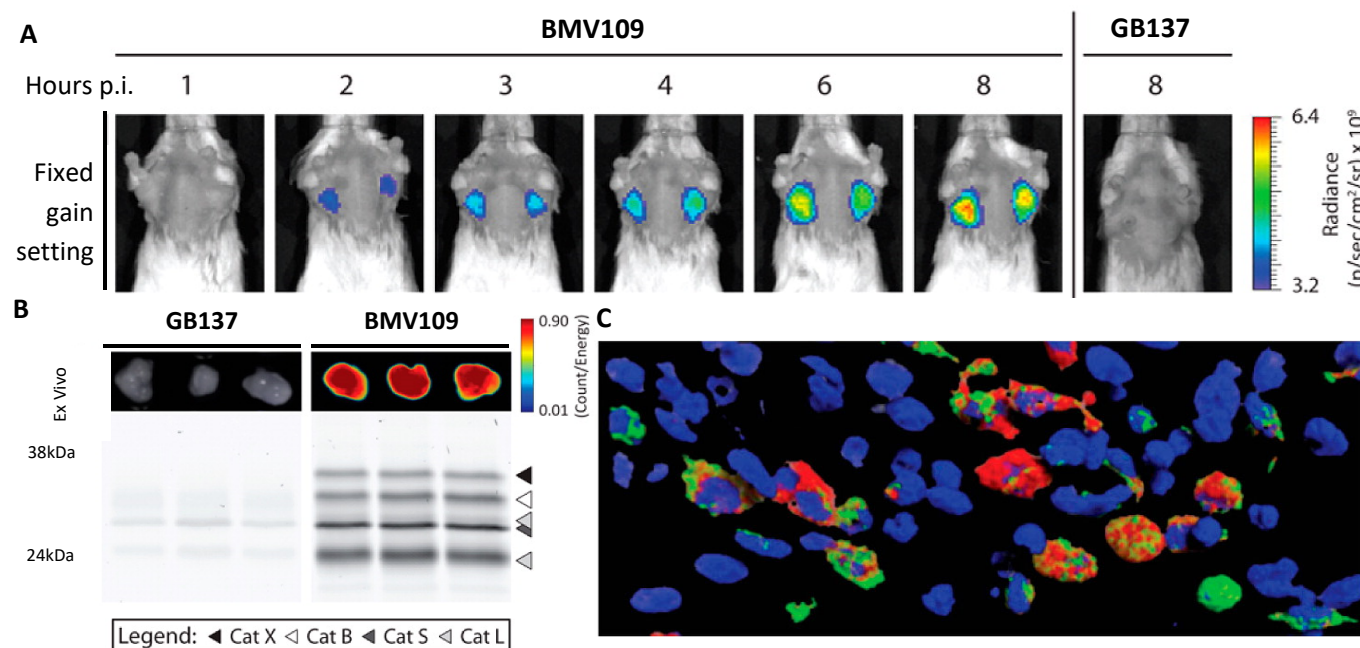


**Fig. 7** *In vivo* imaging of breast cancer using cathepsin-targeting quenched activity-based probes (qABPs). (A) Time-course *in vivo* fluorescence imaging of a syngeneic orthotopic mouse model of breast cancer using qABP **BMV109** or **GB137** (p.i. = post-injection). (B) Fluorescence imaging of resected tumours (top panel) and in-gel fluorescent SDS-PAGE of tumour lysates (lower panel). (C) Confocal laser scanning microscopy (CLSM) of a resected tumour tissue section treated with **BMV109** (red) and immunostaining for macrophage marker CD68 (green) and nuclei (DAPI, blue). Adapted from Ref. 152 with permission. Copyright (2013) American Chemical Society.

**BMV157**, have been used in *in vivo* imaging models. **BMV083** showed stronger tumour-localized cathepsin activity than pan-cathepsin qABP **GB137**, as well as selective distribution among organs possessing high cathepsin activity.<sup>151</sup> **BMV157** was used in a syngeneic orthotopic murine breast cancer 4T1 model.<sup>154</sup> The tumour-detection performances of the polymer-based FRET probe **ProSense 680** (Table 1, Fig. 3B) and the unquenched ABP **GB138** were compared in autochthonous mouse colon cancer models using *in vivo* endoscopy or *ex vivo* exposed tissue analysis.<sup>215</sup> The polymer FRET probe revealed smaller lesions not labeled by the ABP, suggesting differences in biodistribution and overall signal generation.<sup>215</sup> Considerations and best practices for using cathepsin-targeted qABPs in mouse models of cancer are detailed elsewhere.<sup>217</sup>

While less common, fluorogenic probes have also found applications in *in vivo* imaging. The fluorogenic probe **Z-FR-HMRG** used in endoscopy detected tumours in the abdominal cavities of mice.<sup>73</sup> Future work used the probe to image the localization of peritoneally implanted SHIN3 and SKOV-3 tumour cells in mice, albeit invasively.<sup>218</sup> The binding-based, Cy5-labeled DARPIn **8h6** was also used for *in vivo* imaging of orthotopic breast cancer in mice.<sup>59</sup>

Dual-modality probes for cysteine cathepsins have also been used for *in vivo* cancer imaging, such as the dual-modality NIRF(Cy5)/PET(<sup>64</sup>Cu) probe **<sup>64</sup>Cu-GB170**, which was used for optical and PET imaging of subcutaneous tumours in mice.<sup>149</sup> A dual-modal PET/fluorescence cathepsin ABP, **<sup>90</sup>Y-BMX2** (Table 1), bearing a <sup>90</sup>Y radiolabel, was characterized with *in vivo* mouse xenograft models.<sup>219</sup> The PET signal was used to monitor tumour growth and survival rate, while optical imaging was used to determine tumour uptake of the probe.<sup>219</sup> Further

multimodal imaging and theranostic probes could have benefits and have been considered for other protease targets.<sup>184</sup>

Theranostic polymer probes have demonstrated utility for *in vivo* imaging and PDT treatment of either flank tumours using **L-SR15**<sup>135</sup> (Table 1, Fig. 3B) or **CRUN**,<sup>88</sup> and 4T1 breast tumours using **YBN14**<sup>157, 158</sup> in mice.

#### *In vivo* imaging of other pathologies

The involvement of cathepsins in many pathologies merits their use as biomarkers for many of these diseases.<sup>7</sup> Cathepsins contribute to inflammatory processes and cathepsin probes have been used to image inflamed tissues.<sup>5</sup>

Inflammation in various cardiovascular diseases has been imaged extensively using cathepsin probes, including early aortic valve disease<sup>220</sup> and atherosclerosis.<sup>221</sup> A dual-modality PET/fluorescence probe **<sup>64</sup>Cu-BMV101** was used to image vascular inflammation (Fig. 8A).<sup>147</sup> ProSense probes have been used extensively in cardiovascular diseases including myocardial infarction<sup>222</sup> and atherosclerosis,<sup>10, 223</sup> and have even enabled fluorescence lifetime imaging of myocardial infarction *in vivo* in mice.<sup>224</sup> In two examples, theranostic cathepsin probes **L-SR15** (a polymer FRET probe)<sup>136</sup> and **YBN14** (qABP)<sup>158</sup> were used to image and treat mouse models of atherosclerosis in various stages of progression invasively and non-invasively, respectively.

**GB123** (ABP) and **GB137** (qABP) were used in colitis and hyperalgesia models, measuring the contribution of CTS to inflammatory pain.<sup>225</sup> The CTS-selective FRET probe **AW-091** was used to detect inflammation in an *in vivo* mouse model of paw inflammation,<sup>119</sup> and a similar paw model of rheumatoid arthritis was imaged *in vivo* using a ProSense probe.<sup>226</sup> ProSense probes have also been used to assess cathepsin activity in many

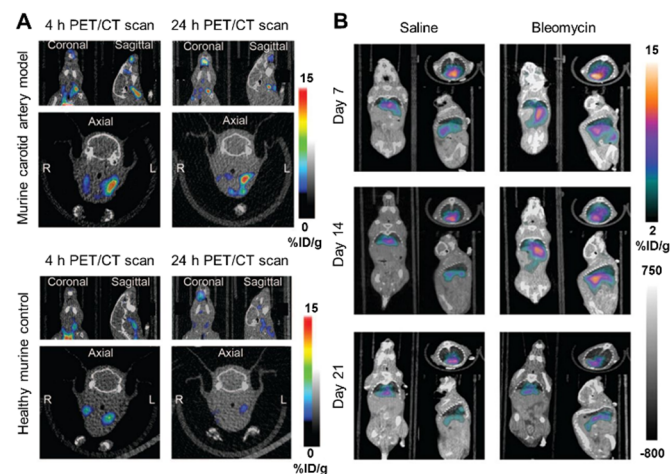


**Fig. 8.** PET imaging of cathepsin activity in inflammation and fibrosis. (A) *In vivo* imaging of macrophage-rich carotid lesions in diabetic or healthy mice, using the pan-cathepsin dual optical/PET imaging ABP <sup>64</sup>Cu-BMV101. In both groups the left carotid artery was ligated to induce macrophage-rich thickening of the vessel walls. Adapted from Ref. 147 with permission. Copyright (2016) SNMMI. (B) *In vivo* imaging of bleomycin-induced idiopathic pulmonary fibrosis using <sup>64</sup>Cu-BMV101. PET/CT scans of mice 7, 14, and 21 days after induction of pulmonary fibrosis. Images are of coronal (left), transaxial (top right) and sagittal (bottom right) perspectives. Adapted from Ref. 148 with permission. Copyright (2016) Nature Publishing Group.

other inflammatory processes, including asthma<sup>227</sup> and immune cell response during rejection of transplanted hearts in mice.<sup>228</sup> Reflecting the significance of CTK activity to osteoporosis,<sup>57, 58</sup> a CTK-selective ProSense probe was successfully used to image osteoclast activity in mice.<sup>11</sup> The FRET probe **6QC-NIR** was recently applied to *in vivo* imaging of middle-ear inflammation during otitis media.<sup>116</sup> A variety of cathepsin-responsive polymer FRET probes have been applied in inflammatory models of colitis.<sup>229</sup> The inflammatory processes during pulmonary fibrosis were monitored by non-invasive whole-body PET imaging using <sup>64</sup>Cu-BMV101 (Fig. 8B).<sup>5, 148</sup> The probe progressed to clinical trials for patients with idiopathic pulmonary fibrosis (NCT02485886) between 2015-2017.

#### **Ex vivo and in vivo imaging-guided surgery**

*Ex vivo* analysis is used to study or validate cathepsin expression or activity *in vivo*. Application of cathepsin imaging probes to identify tumour margins was first assessed in mouse models of brain tumours.<sup>230</sup> Topically administered qABP **GB119** (structure not shown<sup>142</sup>) in resected brain tumours tended to label tumour edges but not whole tumour mass and could identify smaller sections of migrating cells, making it conducive to detect tumour margins in surgical contexts.<sup>230</sup> This was supported in brain cancer mouse models and the results were reproduced in clinically resected human glioblastoma multiforme (GBM) tissues.<sup>230</sup> Topical administration lent to a potential surgical protocol of surgical resection – probe application and incubation, visualization of any remaining fluorescence, resection of the remaining fluorescent tumour tissue, then probe application to confirm complete resection.<sup>230</sup> Notably, a prominent portion of the signal was observed in the extracellular space, consistent with the cellular excretion of cathepsins in cancer. The same qABP **GB119** was also used to

visualize healthy tissue margins in excised nonmelanoma skin cancers.<sup>231</sup> In both basal (BCC) and squamous cell carcinomas (SCC), tumour margins were delineated by cathepsin activity to an extent consistent with H&E analysis.

In another study, skin cancer demarcation was performed using fluorogenic probe **6QC-NIR**<sup>112</sup> for excised keratinocyte carcinomas.<sup>114</sup> The clinical protocol developed in this and previous studies<sup>117</sup> provided same-day assessment of tumour margins immediately after excision of skin cancers.<sup>114</sup> In the hands of clinicians trained in the protocol, the fluorescence-based tumour detection method exhibited 62-78% sensitivity and 92-97% specificity.

*Ex vivo* labeling of other tissue resections from patients appears promising, with a general protocol published for use of the pan-cathepsin qABP **BMV109**.<sup>153</sup> The probe was used to image disease margins on fresh-frozen biopsy slices of breast, lung, liver, and pancreatic tumours, and provided high resolution compared to histological staining.<sup>153</sup> Polymer FRET probes have also been used for *ex vivo* imaging of colorectal polyps<sup>232</sup> and sentinel lymph node metastases using a dissection or surgical intervention model.<sup>233</sup> *Ex vivo* analysis is also used to guide future *in vivo* applications. The qABP **BMV109** was used to detect colorectal polyps in a mouse models of intestinal neoplasia and colitis-associated colorectal cancer.<sup>46</sup> *Ex vivo* imaging of the removed intestines confirmed labeling of cancer polyps by both intravenous or intrarectal probe application.<sup>46</sup> Topical application of the probe to fresh-frozen human colon tumour tissues also highlighted tumour vs. normal tissues.

Systemic (intravenous) administration of cathepsin probes has also demonstrated promise in surgical tumour resection during imaging-guided surgery. Intravenous injections were used for the imaging-guided surgery models described above using the **6QC** series<sup>112, 113, 115</sup> and the qABP **VGT-309**.<sup>156</sup> The pan-cathepsin probe **LUM015** (Table 1, Fig. 3A) has shown promise in clinical trials for intravenous administration and detecting residual tumours after resection, as demonstrated for breast tumour lumpectomy.<sup>126</sup> It was characterized in mouse models of colorectal cancer,<sup>127</sup> then was used in tandem with a novel imaging system.<sup>206</sup> A Phase I dosing safety trial began in 2014 (NCT01626066),<sup>128</sup> and a subsequent mouse-human phase 1 co-clinical trial articulated the in-human PK/PD results of the probe.<sup>129</sup> Notably, the higher tumour-to-normal signal ratio was benefited both by probe biodistribution and tumour-specific protease activation, illustrating the significance of the probe structure (PEGylation) and FRET quenching mechanism to accomplishing tumour bed detection.<sup>129</sup> **LUM015** is in a current clinical trial for *ex vivo* specimen imaging from patients undergoing radical prostatectomy for prostate cancer, expected to close in September 2021 (NCT03441464). It is also the subject of current clinical trials for breast cancer (reducing positive margins; Phase III Treatment; NCT03686215, ends 2021), residual breast cancer detection in patients receiving neoadjuvant therapy (Phase II; NCT04440982, ends 2025), detection of gastrointestinal (colorectal, pancreatic, and esophageal adenocarcinomas) cancers via *ex vivo* imaging (Phase I/II Diagnostic; NCT02584244, ends 2021), and

pancreatic cancer (detection of primary pancreatic cancer and peritoneal invasion from primary pancreatic cancer during surgery; NCT04276909, ends 2021). Taken together, these of studies and trials demonstrate the power of cathepsin optical imaging tools to improve surgical outcomes.

### Concluding remarks and perspectives

Cysteine cathepsins have long been considered critical therapeutic targets for many diseases.<sup>59</sup> In spite of drawbacks in inhibitor development,<sup>13</sup> imaging probes for cathepsins show much promise for clinical translation. Cysteine cathepsins remain strong contenders on lists of targets for molecular imaging probes<sup>178</sup> and the most recent probes and applications highlighted in this work justify this optimistic outlook. Notably, cathepsin probes of multiple classes have shown translational promise, with fluorogenic,<sup>73</sup> small-molecule FRET,<sup>128</sup> polymer FRET,<sup>134</sup> and ABPs<sup>156</sup> being considered in pre-clinical and clinical trials. Many of these trials are ongoing and the results will reveal the future work that must be done.

The discrete contribution of cathepsins give demand for selective imaging tools capable of parsing their activity. We have seen powerful examples of the information provided by such probes, including the asymmetrical distribution of CTL and CTB within the cell, two cathepsins that are so commonly caught up together. Selective labeling has also enabled the simultaneous use of multiple cathepsins as biomarkers to discriminate between related diseases. Imaging probes reporting exclusively on active cathepsins also show powerful discrimination, as only certain sub-populations of CTK within a sample may be enzymatically active, a finding that would be overlooked if fluorescent antibodies alone were used.<sup>10</sup>

Cathepsins are useful biomarkers for *in vitro* analyses and basic biomedical research.<sup>184</sup> Quantification of cathepsin activity is a critical mainstay in these fields, and the development of probes that are highly selective while remaining structurally simple and commercially scalable could further simplify routine assays involving cell lysates and clinical sample analysis or high-throughput drug screening without increasing costs significantly.

Considering the most successful applications, cathepsins appear to be appropriate targets for molecular imaging, as their excretion and heavy involvement in tumours and other diseased tissues make them useful markers for close-proximity medical procedures like imaging-guided surgery and *ex vivo* surgical analysis, applications in which optical imaging probes already find their niche.<sup>60</sup>

For systemic imaging, optical imaging probes are held back by their limited tissue penetration depth.<sup>60</sup> However, fluorescent probes have been serving as proxies for the development of advanced medical imaging probes, such as those used in PET and MRI, providing preclinical validation before conversion to the more precious forms.<sup>5, 139, 140, 147-149</sup>

Overall, cysteine cathepsins have proven to be important targets for diagnosing and monitoring many critical pathologies. The current examination of cathepsin imaging probes *in vitro*, in

cells, in research animals, and in clinical trials<sup>178</sup> shows the promise of the targeted imaging strategies summarized here.

### Conflicts of interest

The authors are the inventors of the patent for the probe CTLAP mentioned in this article (Fig. 1A and Table 1).

### Acknowledgements

This work is supported by research grants to Prof. L. Cui from the National Institute of General Medical Sciences of National Institutes of Health (Maximizing Investigators' Research Award for Early Stage Investigators, R35GM124963), the Department of Defense (Congressionally Directed Medical Research Programs Career Development Award, W81XWH-17-1-0529), and the University of Florida (UF Startup Fund), and to K.A. Schleyer from the University of Florida Health Cancer Center (UFHCC Predoctoral Award).

### Notes and references

1. V. Turk, V. Stoka, O. Vasiljeva, M. Renko, T. Sun, B. Turk and D. Turk, *Biochim. Biophys. Acta*, 2012, **1824**, 68-88.
2. T. Tamhane, R. Llukumbura, S. Lu, G. M. Maelandsmo, M. H. Haugen and K. Brix, *Biochimie*, 2016, **122**, 208-218.
3. B. Goulet, L. Sansregret, L. Leduy, M. Bogyo, E. Weber, S. S. Chauhan and A. Nepveu, *Mol. Cancer Res.*, 2007, **5**, 899-907.
4. J. Mai, R. L. Finley, Jr., D. M. Waisman and B. F. Sloane, *J. Biol. Chem.*, 2000, **275**, 12806-12812.
5. E. Vidak, U. Javorsek, M. Vizovisek and B. Turk, *Cells*, 2019, **8**.
6. K. Brix, A. Dunkhorst, K. Mayer and S. Jordans, *Biochimie*, 2008, **90**, 194-207.
7. L. Kramer, D. Turk and B. Turk, *Trends Pharmacol. Sci.*, 2017, **38**, 873-898.
8. J. M. Lankelma, D. M. Voorend, T. Barwari, J. Koetsveld, A. H. Van der Spek, A. P. De Porto, G. Van Rooijen and C. J. Van Noorden, *Life Sci.*, 2010, **86**, 225-233.
9. M. M. Mohamed and B. F. Sloane, *Nat. Rev. Cancer*, 2006, **6**, 764-775.
10. F. A. Jaffer, D. E. Kim, L. Quinti, C. H. Tung, E. Aikawa, A. N. Pande, R. H. Kohler, G. P. Shi, P. Libby and R. Weissleder, *Circulation*, 2007, **115**, 2292-2298.
11. K. M. Kozloff, L. Quinti, S. Patntirapong, P. V. Hauschka, C. H. Tung, R. Weissleder and U. Mahmood, *Bone*, 2009, **44**, 190-198.
12. J. Reiser, B. Adair and T. Reinheckel, *J. Clin. Invest.*, 2010, **120**, 3421-3431.
13. L. Cianni, C. W. Feldmann, E. Gilberg, M. Gutschow, L. Juliano, A. Leitao, J. Bajorath and C. A. Montanari, *J. Med. Chem.*, 2019, **62**, 10497-10525.
14. Y. Choe, F. Leonetti, D. C. Greenbaum, F. Lecaille, M. Bogyo, D. Bromme, J. A. Ellman and C. S. Craik, *J. Biol. Chem.*, 2006, **281**, 12824-12832.

15. M. Vizovisek, R. Vidmar, E. Van Quickenberghe, F. Impens, U. Andjelkovic, B. Sobic, V. Stoka, K. Gevaert, B. Turk and M. Fonovic, *Proteomics*, 2015, **15**, 2479-2490.
16. M. Tholen, J. J. Yim, K. Groborz, E. Yoo, B. A. Martin, N. S. van den Berg, M. Drag and M. Bogyo, *Angew. Chem. Int. Ed.*, 2020, **59**, 19143-19152.
17. H. Y. Hu, S. Gehrig, G. Reither, D. Subramanian, M. A. Mall, O. Plettenburg and C. Schultz, *Biotechnol. J.*, 2014, **9**, 266-281.
18. R. Loser and J. Pietzsch, *Front. Chem.*, 2015, **3**, 37.
19. I. Santamaria, G. Velasco, M. Cazorla, A. Fueyo, E. Campo and C. Lopez-Otin, *Cancer Res.*, 1998, **58**, 1624-1630.
20. D. Bromme, Z. Li, M. Barnes and E. Mehler, *Biochemistry*, 1999, **38**, 2377-2385.
21. G. J. Tan, Z. K. Peng, J. P. Lu and F. Q. Tang, *World J. Biol. Chem.*, 2013, **4**, 91-101.
22. F. H. Drake, R. A. Dodds, I. E. James, J. R. Connor, C. Deboucq, S. Richardson, E. Lee-Ryckaczewski, L. Coleman, D. Rieman, R. Barthlow, G. Hastings and M. Gowen, *J. Biol. Chem.*, 1996, **271**, 12511-12516.
23. G. P. Shi, A. C. Webb, K. E. Foster, J. H. M. Knoll, C. A. Lemere, J. S. Munger and H. A. Chapman, *J. of Biol. Chem.*, 1994, **269**, 11530-11536.
24. K. Brix, J. McInnes, A. Al-Hashimi, M. Rehders, T. Tamhane and M. H. Haugen, *Protoplasma*, 2015, **252**, 755-774.
25. O. C. Olson and J. A. Joyce, *Nat. Rev. Cancer*, 2015, **15**, 712-729.
26. J. Rozhin, M. Sameni, G. Ziegler and B. F. Sloan, *Cancer Res.*, 1994, **54**, 6517-6525.
27. D. Yan, H. W. Wang, R. L. Bowman and J. A. Joyce, *Cell Rep.*, 2016, **16**, 2914-2927.
28. F. Lecaille, Y. Choe, W. Brandt, Z. Li, C. S. Craik and D. Brömme, *Biochemistry*, 2002, **41**, 8447-8454.
29. F. Fan, S. Nie, E. B. Dammer, D. M. Duong, D. Pan, L. Ping, L. Zhai, J. Wu, X. Hong, L. Qin, P. Xu and Y. H. Zhang, *J. Proteome Res.*, 2012, **11**, 5763-5772.
30. M. L. Biniossek, D. K. Nagler, C. Becker-Pauly and O. Schilling, *J. Proteome Res.*, 2011, **10**, 5363-5373.
31. M. Fonovic and B. Turk, *Biochim. Biophys. Acta*, 2014, **1840**, 2560-2570.
32. O. Vasiljeva, A. Papazoglou, A. Kruger, H. Brodoefel, M. Korovin, J. Deussing, N. Augustin, B. S. Nielsen, K. Almholt, M. Bogyo, C. Peters and T. Reinheckel, *Cancer Res.*, 2006, **66**, 5242-5250.
33. I. Abd-Elrahman, K. Meir, H. Kosuge, Y. Ben-Nun, T. Weiss Sadan, C. Rubinstein, Y. Samet, M. V. McConnell and G. Blum, *Stroke*, 2016, **47**, 1101-1108.
34. S. Kitamoto, G. K. Sukhova, J. Sun, M. Yang, P. Libby, V. Love, P. Duramad, C. Sun, Y. Zhang, X. Yang, C. Peters and G. P. Shi, *Circulation*, 2007, **115**, 2065-2075.
35. T. Reinheckel, S. Hagemann, S. Dollwet-Mack, E. Martinez, T. Lohmuller, G. Zlatkovic, D. J. Tobin, N. Maas-Szabowski and C. Peters, *J. Cell Sci.*, 2005, **118**, 3387-3395.
36. J. Dennemarker, T. Lohmuller, J. Mayerle, M. Tacke, M. M. Lerch, L. M. Coussens, C. Peters and T. Reinheckel, *Oncogene*, 2010, **29**, 1611-1621.
37. C. Lopez-Otin and L. M. Matrisian, *Nat. Rev. Cancer*, 2007, **7**, 800-808.
38. S. Mehra, R. Panwar, B. Thakur, R. Yadav, M. Kumar, R. Singh, N. R. Dash, P. Sahni and S. S. Chauhan, *Front. Oncol.*, 2019, **9**, 1239.
39. N. Singh, P. Das, S. Gupta, V. Sachdev, S. Srivasatava, S. Datta Gupta, R. M. Pandey, P. Sahni, S. S. Chauhan and A. Saraya, *World J. Gastroenterol.*, 2014, **20**, 17532-17540.
40. T. T. Lah, M. Cercek, A. Blejec, J. Kos, E. Gorodetsky, R. Somers and I. Daskal, *Clin. Cancer Res.*, 2000, **6**, 578-584.
41. A. M. Troy, K. Sheahan, H. E. Mulcahy, M. J. Duffy, J. M. Hyland and D. P. O'Donoghue, *Eur. J. Cancer*, 2004, **40**, 1610-1616.
42. Y. Bauer, P. Hess, C. Qiu, A. Klenk, B. Renault, D. Wanner, R. Studer, N. Killer, A. K. Stalder, M. Stritt, D. S. Strasser, H. Farine, K. Kauser, M. Clozel, W. Fischli and O. Nayler, *Hypertension*, 2011, **57**, 795-801.
43. G. Pandey, S. Bakhshi, B. Thakur, P. Jain and S. S. Chauhan, *Leuk. Lymphoma*, 2018, **59**, 2175-2187.
44. Y. Liu, X. Li, D. Peng, Z. Tan, H. Liu, Y. Qing, Y. Xue and G. P. Shi, *Am. J. Cardiol.*, 2009, **103**, 476-481.
45. Y. Cao, X. Liu, Y. Li, Y. Lu, H. Zhong, W. Jiang, A. F. Chen, T. R. Billiar, H. Yuan and J. Cai, *Int. Urol. Nephrol.*, 2017, **49**, 1409-1417.
46. E. Segal, T. R. Prestwood, W. A. van der Linden, Y. Carmi, N. Bhattacharya, N. Withana, M. Verdoes, A. Habtezion, E. G. Engleman and M. Bogyo, *Chem. Biol.*, 2015, **22**, 148-158.
47. S. D. Mason and J. A. Joyce, *Trends Cell Biol.*, 2011, **21**, 228-237.
48. P. Libby, J. E. Buring, L. Badimon, G. K. Hansson, J. Deanfield, M. S. Bittencourt, L. Tokgozoglu and E. F. Lewis, *Nat Rev Dis Primers*, 2019, **5**, 56.
49. S. P. Lutgens, K. B. Cleutjens, M. J. Daemen and S. Heeneman, *FASEB J.*, 2007, **21**, 3029-3041.
50. D. Buccheri, D. Piraino, G. Andolina and B. Cortese, *J. Thorac. Dis.*, 2016, **8**, E1150-E1162.
51. L. Lindstedt, M. Lee, K. Oorni, D. Bromme and P. T. Kovanen, *Biochem. Biophys. Res. Commun.*, 2003, **312**, 1019-1024.
52. D. L. Dinnes, M. Y. White, M. Kockx, M. Traini, V. Hsieh, M. J. Kim, L. Hou, W. Jessup, K. A. Rye, M. Thaysen-Andersen, S. J. Cordwell and L. Kritharides, *FASEB J.*, 2016, **30**, 4239-4255.
53. T. Weiss-Sadan, I. Gotsman and G. Blum, *FEBS J.*, 2017, **284**, 1455-1472.
54. J. Liu, G. K. Sukhova, J. T. Yang, J. Sun, L. Ma, A. Ren, W. H. Xu, H. Fu, G. M. Dolganov, C. Hu, P. Libby and G. P. Shi, *Atherosclerosis*, 2006, **184**, 302-311.
55. J. Liu, L. Ma, J. Yang, A. Ren, Z. Sun, G. Yan, J. Sun, H. Fu, W. Xu, C. Hu and G. P. Shi, *Atherosclerosis*, 2006, **186**, 411-419.
56. S. Taleb, D. Lacasa, J. P. Bastard, C. Poitou, R. Canello, V. Pelloux, N. Viguerie, A. Benis, J. D. Zucker, J. L. Bouillot, C. Coussieu, A. Basdevant, D. Langin and K. Clement, *FASEB J.*, 2005, **19**, 1540-1542.
57. R. Eastell, T. W. O'Neill, L. C. Hofbauer, B. Langdahl, I. R. Reid, D. T. Gold and S. R. Cummings, *Nat Rev Dis Primers*, 2016, **2**, 16069.
58. P. Garnerio, O. Borel, I. Byrjalsen, M. Ferreras, F. H. Drake, M. S. McQueney, N. T. Foged, P. D. Delmas and J. M. Delaisse, *J. Biol. Chem.*, 1998, **273**, 32347-32352.
59. L. Kramer, M. Renko, J. Završnik, D. Turk, M. A. Seeger, O. Vasiljeva, M. G. Grutter, V. Turk and B. Turk, *Theranostics*, 2017, **7**, 2806-2821.
60. M. L. James and S. S. Gambhir, *Physiol. Rev.*, 2012, **92**, 897-965.

61. V. Ntziachristos, A. G. Yodh, M. Schnall and B. Chance, *Proc. Natl. Acad. Sci. USA*, 2000, **97**, 2767-2772.
62. K. R. Tringale, J. Pang and Q. T. Nguyen, *Wiley Interdiscip. Rev. Syst. Biol. Med.*, 2018, **10**, e1412.
63. C. W. Barth and S. L. Gibbs, *Proc. SPIE Int. Soc. Opt. Eng.*, 2020, **11222**.
64. A. L. Vahrmeijer, M. Hutteman, J. R. van der Vorst, C. J. van de Velde and J. V. Frangioni, *Nat Rev Clin Oncol*, 2013, **10**, 507-518.
65. J. Zhang, X. Chai, X. P. He, H. J. Kim, J. Yoon and H. Tian, *Chem. Soc. Rev.*, 2019, **48**, 683-722.
66. L. Wu, C. Huang, B. P. Emery, A. C. Sedgwick, S. D. Bull, X. P. He, H. Tian, J. Yoon, J. L. Sessler and T. D. James, *Chem. Soc. Rev.*, 2020, **49**, 5110-5139.
67. L. E. Edgington, M. Verdoes and M. Bogoyo, *Curr. Opin. Chem. Biol.*, 2011, **15**, 798-805.
68. W. Chyan and R. T. Raines, *ACS Chem. Biol.*, 2018, **13**, 1810-1823.
69. H. W. Liu, L. Chen, C. Xu, Z. Li, H. Zhang, X. B. Zhang and W. Tan, *Chem. Soc. Rev.*, 2018, **47**, 7140-7180.
70. H. M. Burke, T. Gunnlaugsson and E. M. Scanlan, *Chem. Commun.*, 2015, **51**, 10576-10588.
71. K.-i. Setsukinai, Y. Urano, K. Kikuchi, T. Higuchi and T. Nagano, *J. Chem. Soc. Perk. T. 2*, 2000, DOI: 10.1039/b006449l, 2453-2457.
72. K. A. Schleyer, B. Fetrow, P. Z. Fatland, J. Liu, M. Chaaban, B. Ma and L. Cui, *ChemMedChem*, 2020, DOI: 10.1002/cmdc.202000823.
73. T. Fujii, M. Kamiya and Y. Urano, *Bioconjug. Chem.*, 2014, **25**, 1838-1846.
74. B. J. Backes, J. L. Harris, F. Leonetti, C. S. Craik and J. A. Ellman, *Nat. Biotechnol.*, 2000, **18**, 187-193.
75. M. Monici, *Biotechnology Annual Review*, 2005, **11**, 227-256.
76. I. Assfalg-Machleidt, G. Rothe, S. Klingel, R. Banati, W. F. Mangel, G. Valet and W. Machleidt, *Biol. Chem. H.-S.*, 1992, **373**, 433-440.
77. E. Boonacker and C. J. Van Noorden, *J. Histochem. Cytochem.*, 2001, **49**, 1473-1486.
78. Y. Wang, J. Li, L. Feng, J. Yu, Y. Zhang, D. Ye and H. Y. Chen, *Anal. Chem.*, 2016, **88**, 12403-12410.
79. T. Morita, H. Kato, S. Iwanaga, K. Takada and T. Kimura, *J. Biochem.*, 1977, **82**, 1495-1498.
80. A. J. Barrett, *Biochem. J.*, 1980, **187**, 909-912.
81. J. R. Tchoupé, T. Moreau, F. Gauthier and J. G. Bieth, *BBA-Protein Struct. M.*, 1991, **1076**, 149-151.
82. D. J. Maly, F. Leonetti, B. J. Backes, D. S. Dauber, J. L. Harris, C. S. Craik and J. A. Ellman, *J. Org. Chem.*, 2002, **67**, 910-915.
83. J. L. Harris, B. J. Backes, F. Leonetti, S. Mahrus, J. A. Ellman and C. S. Craik, *Proc. Natl. Acad. Sci. USA*, 2000, **97**, 7754-7759.
84. A. P. Castano, T. N. Demidova and M. R. Hamblin, *Photodiagn. Photodyn.*, 2004, **1**, 279-293.
85. J. Mei, N. L. Leung, R. T. Kwok, J. W. Lam and B. Z. Tang, *Chem. Rev.*, 2015, **115**, 11718-11940.
86. Y. Yuan, C. J. Zhang, M. Gao, R. Zhang, B. Z. Tang and B. Liu, *Angew. Chem. Int. Ed.*, 2015, **54**, 1780-1786.
87. G. Liang, H. Ren and J. Rao, *Nat. Chem.*, 2010, **2**, 54-60.
88. X. Ai, C. J. Ho, J. Aw, A. B. Attia, J. Mu, Y. Wang, X. Wang, Y. Wang, X. Liu, H. Chen, M. Gao, X. Chen, E. K. Yeow, G. Liu, M. Olivo and B. Xing, *Nat. Commun.*, 2016, **7**, 10432.
89. M. E. Roth-Konforti, C. R. Bauer and D. Shabat, *Angew. Chem. Int. Ed.*, 2017, **56**, 15633-15638.
90. A. P. Schaap, T.-S. Chen, R. S. Handley, R. DeSilva and B. P. Giri, *Tetrahedron Lett.*, 1987, **28**, 1155-1158.
91. Y. Ni, Z. Hai, T. Zhang, Y. Wang, Y. Yang, S. Zhang and G. Liang, *Anal. Chem.*, 2019, **91**, 14834-14837.
92. R. W. Mason, M. A. J. Taylor and D. J. Etherington, *Biochem J.*, 1984, **217**, 209-217.
93. A. J. Barrett and H. Krirschke, *Method Enzymol.*, 1981, **80**, 535-561.
94. H. Kirschke and B. Wiederanders, *Method Enzymol.*, 1994, **244**, 500-511.
95. R. A. Maciewicz and D. J. Etherington, *Biochem J.*, 1988, **256**, 433-440.
96. D. Cavallo-Medved, D. Rudy, G. Blum, M. Bogoyo, D. Caglic and B. F. Sloane, *Exp. Cell Res.*, 2009, **315**, 1234-1246.
97. M. A. Chowdhury, I. A. Moya, S. Bhilocha, C. C. McMillan, B. G. Vigliarolo, I. Zehbe and C. P. Phenix, *J. Med. Chem.*, 2014, **57**, 6092-6104.
98. M. Poreba, K. Groborz, M. Vizovisek, M. Maruggi, D. Turk, B. Turk, G. Powis, M. Drag and G. S. Salvesen, *Chem. Sci.*, 2019, **10**, 8461-8477.
99. M. Poreba, W. Rut, M. Vizovisek, K. Groborz, P. Kasperkiewicz, D. Finlay, K. Vuori, D. Turk, B. Turk, G. S. Salvesen and M. Drag, *Chem. Sci.*, 2018, **9**, 2113-2129.
100. S. Chen, S. Lovell, S. Lee, M. Fellner, P. D. Mace and M. Bogoyo, *Nat. Biotechnol.*, 2020, DOI: 10.1038/s41587-020-0733-7.
101. M. Bogoyo, Putting phage to work for covalent inhibitor design, <https://bioengineeringcommunity.nature.com/posts/putting-phage-to-work-for-covalent-inhibitor-design>, (accessed December 17, 2020, 2020).
102. I. Schechter and A. Berger, *Biochem. Biophys. Res. Commun.*, 1967, **27**, 157-162.
103. F. Lecaille, E. Weidauer, M. A. Juliano, D. Bromme and G. Lalmanach, *Biochem J.*, 2003, **375**, 307-312.
104. M. F. Alves, L. Puzer, S. S. Cotrin, M. A. Juliano, L. Juliano, D. Bromme and A. K. Carmona, *Biochem J.*, 2003, **373**, 981-986.
105. A. Vaithilingam, N. Y. Lai, E. Duong, J. Boucau, Y. Xu, M. Shimada, M. Gandhi and S. Le Gall, *BMC Cell Biol.*, 2013, **14**, 35.
106. R. C. Kamboj, S. Pal, N. Raghav and H. Singh, *Biochimie*, 1993, **75**, 873-878.
107. A. Torkar, B. Lenarcic, T. Lah, V. Dive and L. Devel, *Bioorg. Med. Chem. Lett.*, 2013, **23**, 2968-2973.
108. K. A. Schleyer, B. Fetrow, P. Z. Fatland, J. Liu, M. Chaaban, B. Ma and L. Cui, *ChemMedChem*, 2020, DOI: 10.1002/cmdc.202000823.
109. Y. Wang, J. Li, L. Feng, J. Yu, Y. Zhang, D. Ye and H. Y. Chen, *Anal. Chem.*, 2016, **88**, 12403-12410.
110. T. Fujii, M. Kamiya and Y. Urano, *Bioconjugate Chem.*, 2014, **25**, 1838-1846.
111. G. M. Dubowchik, R. A. Firestone, L. Padilla, D. Willner, S. J. Hofstead, K. Mosure, J. O. Knipe, S. J. Lasch and P. A. Trail, *Bioconjugate Chem.*, 2002, **13**, 855-869.
112. L. O. Ofori, N. P. Withana, T. R. Prestwood, M. Verdoes, J. J. Brady, M. M. Winslow, J. Sorger and M. Bogoyo, *ACS Chem. Biol.*, 2015, **10**, 1977-1988.
113. J. J. Yim, M. Tholen, A. Klaassen, J. Sorger and M. Bogoyo, *Mol. Pharm.*, 2018, **15**, 750-758.

114. E. Walker, Y. Liu, I. Kim, M. Biro, S. R. Iyer, H. Ezaldein, J. Scott, M. Merati, R. Mistur, B. Zhou, B. Straight, J. J. Yim, M. Bogyo, M. Mann, D. L. Wilson, J. P. Basilion and D. L. Popkin, *Cancer Res.*, 2020, **80**, 2045-2055.
115. J. J. Yim, S. Harmsen, K. Flisikowski, T. Flisikowska, H. Namkoong, M. Garland, N. S. van den Berg, J. G. Vilches-Moure, A. Schnieke, D. Saur, S. Glasl, D. Gorpas, A. Habtezion, V. Ntziachristos, C. H. Contag, S. S. Gambhir, M. Bogyo and S. Rogalla, *Proc. Natl. Acad. Sci. USA*, 2021, **118**.
116. J. J. Yim, S. P. Singh, A. Xia, R. Kashfi-Sadabad, M. Tholen, D. M. Huland, D. Zarabanda, Z. Cao, P. Solis-Pazmino, M. Bogyo and T. A. Valdez, *ACS Sens.*, 2020, **5**, 3411-3419.
117. Y. Liu, E. Walker, S. R. Iyer, M. Biro, I. Kim, B. Zhou, B. Straight, M. Bogyo, J. P. Basilion, D. L. Popkin and D. L. Wilson, *J. Med. Imaging*, 2019, **6**, 016001.
118. J. C. Widen, M. Tholen, J. J. Yim, A. Antaris, K. M. Casey, S. Rogalla, A. Klaassen, J. Sorger and M. Bogyo, *Nat. Biomed. Eng.*, 2020, DOI: 10.1038/s41551-020-00616-6.
119. D. Caglic, A. Globisch, M. Kindermann, N. H. Lim, V. Jeske, H. P. Juretschke, E. Bartnik, K. U. Weithmann, H. Nagase, B. Turk and K. U. Wendt, *Bioorg. Med. Chem.*, 2011, **19**, 1055-1061.
120. Y. J. Zhong, L. H. Shao and Y. Li, *Int. J. Oncol.*, 2013, **42**, 373-383.
121. A. Satsangi, S. S. Roy, R. K. Satsangi, R. K. Vadlamudi and J. L. Ong, *Mol. Pharm.*, 2014, **11**, 1906-1918.
122. X. Chen, D. Lee, S. Yu, G. Kim, S. Lee, Y. Cho, H. Jeong, K. T. Nam and J. Yoon, *Biomaterials*, 2017, **122**, 130-140.
123. R. Tian, M. Li, J. Wang, M. Yu, X. Kong, Y. Feng, Z. Chen, Y. Li, W. Huang, W. Wu and Z. Hong, *Org. Biomol. Chem.*, 2014, **12**, 5365-5374.
124. H. Y. Hu, D. Vats, M. Vizovisek, L. Kramer, C. Germanier, K. U. Wendt, M. Rudin, B. Turk, O. Plettenburg and C. Schultz, *Angew. Chem. Int. Ed.*, 2014, **53**, 7669-7673.
125. M. Legowska, M. Wysocka, T. Burster, M. Pikula, K. Rolka and A. Lesner, *Anal. Biochem.*, 2014, **466**, 30-37.
126. B. L. Smith, M. A. Gadd, C. R. Lanahan, U. Rai, R. Tang, T. Rice-Stitt, A. L. Merrill, D. B. Strasfeld, J. M. Ferrer, E. F. Brachtel and M. C. Specht, *Breast Cancer Res. Treat.*, 2018, **171**, 413-420.
127. S. A. Esfahani, P. Heidari, M. H. Kucherlapati, J. M. Ferrer, R. S. Kucherlapati and U. Mahmood, *Am. J. Nucl. Med. Mol. Imaging*, 2019, **9**, 230-242.
128. M. J. Whitley, D. M. Cardona, D. G. Blazer, S. E. Hwang, P. J. Mosca, J. Cahill, J. M. Ferrer, D. B. Strasfeld, J. K. Mito, K. C. Cuneo, N. Larrier, N. Williams, I. Spasojevic, R. F. Riedel, W. Eward, W. D. Lee, L. G. Griffith, M. Bawendi, D. G. Kirsch and B. E. Brigman, *J. of Clin. Oncol.*, 2014, **32**, TPS11135-TPS11135.
129. M. J. Whitley, D. M. Cardona, A. L. Lazarides, I. Spasojevic, J. M. Ferrer, J. Cahill, C. L. Lee, M. Snuderl, D. G. Blazer, 3rd, E. S. Hwang, R. A. Greenup, P. J. Mosca, J. K. Mito, K. C. Cuneo, N. A. Larrier, E. K. O'Reilly, R. F. Riedel, W. C. Eward, D. B. Strasfeld, D. Fukumura, R. K. Jain, W. D. Lee, L. G. Griffith, M. G. Bawendi, D. G. Kirsch and B. E. Brigman, *Sci. Transl. Med.*, 2016, **8**, 320ra324.
130. M. Wartenberg, A. Saidi, M. Galibert, A. Joulin-Giet, J. Burlaud-Gaillard, F. Lecaille, C. J. Scott, V. Aucagne, A. F. Delmas and G. Lalmanach, *Biochimie*, 2019, **166**, 84-93.
131. Q. Wang, L. Yu, R. C. H. Wong and P. C. Lo, *Eur. J. Med. Chem.*, 2019, **179**, 828-836.
132. A. Watzke, G. Kosec, M. Kindermann, V. Jeske, H. P. Nestler, V. Turk, B. Turk and K. U. Wendt, *Angew. Chem. Int. Ed.*, 2008, **47**, 406-409.
133. U. Mahmood, C. H. Tung, A. Bogdanov, Jr. and R. Weissleder, *Radiology*, 1999, **213**, 866-870.
134. R. Weissleder, C. H. Tung, U. Mahmood and A. Bogdanov, Jr., *Nat. Biotechnol.*, 1999, **17**, 375-378.
135. Y. Choi, R. Weissleder and C. H. Tung, *Cancer Res.*, 2006, **66**, 7225-7229.
136. S. M. Shon, Y. Choi, J. Y. Kim, D. K. Lee, J. Y. Park, D. Schellingerhout and D. E. Kim, *Arterioscler. Thromb. Vasc. Biol.*, 2013, **33**, 1360-1365.
137. C. H. Tung, U. Mahmood, S. Bredow and R. Weissleder, *Cancer Res*, 2000, **60**, 4953-4958.
138. A. T. N. Kumar, W. L. Rice, J. C. Lopez, S. Gupta, C. J. Goergen and A. A. Bogdanov, Jr., *ACS Sens.*, 2016, **1**, 427-436.
139. D. V. Hingorani, L. A. Montano, E. A. Randtke, Y. S. Lee, J. Cardenas-Rodriguez and M. D. Pagel, *Contrast Media Mol. Imaging*, 2016, **11**, 130-138.
140. M. Haris, A. Singh, I. Mohammed, R. Ittyerah, K. Nath, R. P. Nanga, C. Debrosse, F. Kogan, K. Cai, H. Poptani, D. Reddy, H. Hariharan and R. Reddy, *Sci. Rep.*, 2014, **4**, 6081.
141. G. Blum, S. R. Mullins, K. Keren, M. Fonovic, C. Jedeszko, M. J. Rice, B. F. Sloane and M. Bogyo, *Nat. Chem. Biol.*, 2005, **1**, 203-209.
142. G. Blum, G. von Degenfeld, M. J. Merchant, H. M. Blau and M. Bogyo, *Nat. Chem. Biol.*, 2007, **3**, 668-677.
143. L. Ben-Aderet, E. Merquiol, D. Fahham, A. Kumar, E. Reich, Y. Ben-Nun, L. Kandel, A. Haze, M. Liebergall, M. K. Kosinska, J. Steinmeyer, B. Turk, G. Blum and M. Dvir-Ginzberg, *Arthritis Res. Ther.*, 2015, **17**, 69.
144. M. Huisman, J. P. Kodanko, K. Arora, M. Herroon, M. Alnaed, J. Endicott, I. Podgorski and J. J. Kodanko, *Inorg. Chem.*, 2018, **57**, 7881-7891.
145. S. J. Mountford, B. M. Anderson, B. Xu, E. S. V. Tay, M. Szabo, M. L. Hoang, J. Diaol, L. Aurelio, R. I. Campden, E. Lindstrom, E. K. Sloan, R. M. Yates, N. W. Bunnett, P. E. Thompson and L. E. Edgington-Mitchell, *ACS Chem. Biol.*, 2020, **15**, 718-727.
146. A. Torkar, S. Bregant, L. Devel, M. Novinec, B. Lenarcic, T. Lah and V. Dive, *ChemBioChem*, 2012, **13**, 2616-2621.
147. N. P. Withana, T. Saito, X. Ma, M. Garland, C. Liu, H. Kosuge, M. Amsallem, M. Verdoes, L. O. Ofori, M. Fischbein, M. Arakawa, Z. Cheng, M. V. McConnell and M. Bogyo, *J. Nucl. Med.*, 2016, **57**, 1583-1590.
148. N. P. Withana, X. Ma, H. M. McGuire, M. Verdoes, W. A. van der Linden, L. O. Ofori, R. Zhang, H. Li, L. E. Sanman, K. Wei, S. Yao, P. Wu, F. Li, H. Huang, Z. Xu, P. J. Wolters, G. D. Rosen, H. R. Collard, Z. Zhu, Z. Cheng and M. Bogyo, *Sci. Rep.*, 2016, **6**, 19755.
149. G. Ren, G. Blum, M. Verdoes, H. Liu, S. Syed, L. E. Edgington, O. Gheysens, Z. Miao, H. Jiang, S. S. Gambhir, M. Bogyo and Z. Cheng, *PLoS One*, 2011, **6**, e28029.
150. X. W. Ma, X. Li, S. L. Wang, J. Wang and Y. H. Wang, *Journal of Nuclear Medicine*, 2019, **60**.
151. M. Verdoes, L. E. Edgington, F. A. Scheeren, M. Leyva, G. Blum, K. Weiskopf, M. H. Bachmann, J. A. Ellman and M. Bogyo, *Chem. Biol.*, 2012, **19**, 619-628.

152. M. Verdoes, K. Oresic Bender, E. Segal, W. A. van der Linden, S. Syed, N. P. Withana, L. E. Sanman and M. Bogyo, *J. Am. Chem. Soc.*, 2013, **135**, 14726-14730.
153. N. P. Withana, M. Garland, M. Verdoes, L. O. Ofori, E. Segal and M. Bogyo, *Nat Protoc*, 2016, **11**, 184-191.
154. K. Oresic Bender, L. Ofori, W. A. van der Linden, E. D. Mock, G. K. Datta, S. Chowdhury, H. Li, E. Segal, M. Sanchez Lopez, J. A. Ellman, C. G. Figdor, M. Bogyo and M. Verdoes, *J. Am. Chem. Soc.*, 2015, **137**, 4771-4777.
155. L. E. Sanman, W. A. van der Linden, M. Verdoes and M. Bogyo, *Cell Chem. Biol.*, 2016, **23**, 793-804.
156. F. V. Suurs, S. Q. Qiu, J. J. Yim, C. P. Schroder, H. Timmer-Bosscha, E. S. Bensen, J. T. Santini, Jr., E. G. E. de Vries, M. Bogyo and G. M. van Dam, *EJNMMI Res.*, 2020, **10**, 111.
157. Y. Ben-Nun, E. Merquiol, A. Brandis, B. Turk, A. Scherz and G. Blum, *Theranostics*, 2015, **5**, 847-862.
158. T. Weiss-Sadan, Y. Ben-Nun, D. Maimoun, E. Merquiol, I. Abd-Elrahman, I. Gotsman and G. Blum, *Theranostics*, 2019, **9**, 5731-5738.
159. J. Yan, S. Lee, A. Zhang and J. Yoon, *Chem. Soc. Rev.*, 2018, **47**, 6900-6916.
160. A. Alouane, R. Labruere, T. Le Saux, F. Schmidt and L. Jullien, *Angew. Chem. Int. Ed.*, 2015, **54**, 7492-7509.
161. E. Kisin-Finfer, S. Ferber, R. Blau, R. Satchi-Fainaro and D. Shabat, *Bioorg. Med. Chem. Lett.*, 2014, **24**, 2453-2458.
162. J. R. Lakowicz, *Principles of Fluorescence Spectroscopy*, Springer, Third Edition edn., 2006.
163. J. Y. Yhee, S. A. Kim, H. Koo, S. Son, J. H. Ryu, I. C. Youn, K. Choi, I. C. Kwon and K. Kim, *Theranostics*, 2012, **2**, 179-189.
164. Z. Na, L. Li, M. Uttamchandani and S. Q. Yao, *Chem. Commun.*, 2012, **48**, 7304-7306.
165. J. Tian, L. Ding, Q. Wang, Y. Hu, L. Jia, J. S. Yu and H. Ju, *Anal. Chem.*, 2015, **87**, 3841-3848.
166. I. Y. Hirata, M. H. Sedenho Cezari, C. R. Nakaie, P. Boschcov, A. S. Ito, M. A. Juliano and L. Juliano, *Lett. Pept. Sci.*, 1995, **1**, 299-308.
167. N. Marks, M. J. Berg and W. Danho, *Peptides*, 1989, **10**, 391-394.
168. S. Wang, B. G. Vigliarolo, M. A. Chowdhury, J. N. K. Nyarko, D. D. Mousseau and C. P. Phenix, *Bioorg. Chem.*, 2019, **92**, 103194.
169. S. S. Cotrin, L. Puzer, W. A. de Souza Judice, L. Juliano, A. K. Carmona and M. A. Juliano, *Anal. Biochem.*, 2004, **335**, 244-252.
170. M. Oliveira, R. J. Torquato, M. F. Alves, M. A. Juliano, D. Bromme, N. M. Barros and A. K. Carmona, *Peptides*, 2010, **31**, 562-567.
171. C. J. Kim, D. I. Lee, D. Zhang, C. H. Lee and I. S. Ahn, *Anal. Biochem.*, 2013, **435**, 166-173.
172. U. Grabowski, T. J. Chambers and M. Shiroo, *Curr. Opin. Drug Discov. Devel.*, 2005, **8**, 619-630.
173. J. Link and S. Zipfel, *Eupore PMC*, 2006, **9**, 471-482.
174. N. G. Zhegalova, S. He, H. Zhou, D. M. Kim and M. Y. Berezin, *Contrast Media Mol. Imaging*, 2014, **9**, 355-362.
175. C. H. Tung, U. Mahmood, S. Bredow and R. Weissleder, *Cancer Res.*, 2000, **60**, 4953-4958.
176. M. P. Melancon, W. Wang, Y. Wang, R. Shao, X. Ji, J. G. Gelovani and C. Li, *Pharm. Res.*, 2007, **24**, 1217-1224.
177. J. H. Ryu, J. H. Na, H. K. Ko, D. G. You, S. Park, E. Jun, H. J. Yeom, D. H. Seo, J. H. Park, S. Y. Jeong, I. S. Kim, B. S. Kim, I. C. Kwon, K. Choi and K. Kim, *Biomaterials*, 2014, **35**, 2302-2311.
178. M. Garland, J. J. Yim and M. Bogyo, *Cell Chem. Biol.*, 2016, **23**, 122-136.
179. V. Nikolettou, M. Markaki, K. Palikaras and N. Tavernarakis, *Biochim. Biophys. Acta*, 2013, **1833**, 3448-3459.
180. J. Wahsner, E. M. Gale, A. Rodriguez-Rodriguez and P. Caravan, *Chem. Rev.*, 2019, **119**, 957-1057.
181. A. B. Berger, P. M. Vitorino and M. Bogyo, *Am. J. Pharmacogenomic*, 2004, **4**, 371-381.
182. C. M. Kam, A. S. Abuelyaman, Z. Li, D. Hudig and J. C. Powers, *Bioconjug. Chem.*, 1993, **4**, 560-567.
183. L. E. Sanman and M. Bogyo, *Annu. Rev. Biochem.*, 2014, **83**, 249-273.
184. C. S. Hughes, R. E. Burden, B. F. Gilmore and C. J. Scott, *Biochimie*, 2016, **122**, 48-61.
185. J. C. Powers, J. L. Asgian, Ö. D. Ekici and K. E. James, *Chem. Rev.*, 2002, **102**, 4639-4750.
186. M. Frizler, M. D. Mertens and M. Gutschow, *Bioorg. Med. Chem. Lett.*, 2012, **22**, 7715-7718.
187. M. Frizler, I. V. Yampolsky, M. S. Baranov, M. Stirnberg and M. Gutschow, *Org. Biomol. Chem.*, 2013, **11**, 5913-5921.
188. M. D. Mertens, J. Schmitz, M. Horn, N. Furtmann, J. Bajorath, M. Mares and M. Gutschow, *Chembiochem*, 2014, **15**, 955-959.
189. R. A. Smith, L. J. Copp, P. J. Coles, H. W. Pauls, V. J. Robinson, R. W. Spencer, S. B. Heard and A. Krantz, *J. Am. Chem. Soc.*, 1988, **110**, 4429-4431.
190. A. E. Speers, G. C. Adam and B. F. Cravatt, *J. Am. Chem. Soc.*, 2003, **125**, 4686-4687.
191. A. Fernandez and M. Vendrell, *Chem. Soc. Rev.*, 2016, **45**, 1182-1196.
192. R. Loser, R. Bergmann, M. Frizler, B. Mosch, L. Dombrowski, M. Kuchar, J. Steinbach, M. Gutschow and J. Pietzsch, *ChemMedChem*, 2013, **8**, 1330-1344.
193. E. L. Vodovozova, *Biochemistry (Mosc)*, 2007, **72**, 1-20.
194. M. G. Paulick and M. Bogyo, *ACS Chem. Biol.*, 2011, **6**, 563-572.
195. N. Katunuma, E. Murata, H. Kakegawa, A. Matsui, H. Tsuzuki, H. Tsuge, D. Turk, V. Turk, M. Fukushima, Y. Tada and T. Asao, *FEBS Lett.*, 1999, **458**, 6-10.
196. N. Katunuma, *Proc. Jpn. Acad. Ser. B Phys. Biol. Sci.*, 2011, **87**, 29-39.
197. M. Y. Berezin and S. Achilefu, *Chem. Rev.*, 2010, **110**, 2641-2684.
198. N. P. Withana, X. Ma, H. M. McGuire, M. Verdoes, W. A. van der Linden, L. O. Ofori, R. Zhang, H. Li, L. E. Sanman, K. Wei, S. Yao, P. Wu, F. Li, H. Huang, Z. Xu, P. J. Wolters, G. D. Rosen, H. R. Collard, Z. Zhu, Z. Cheng and M. Bogyo, *Sci Rep*, 2016, **6**, 19755.
199. G. Blum, R. M. Weimer, L. E. Edgington, W. Adams and M. Bogyo, *PLoS One*, 2009, **4**, e6374.
200. B. M. Creasy, C. B. Hartmann, F. K. White and K. L. McCoy, *Cytometry A*, 2007, **71**, 114-123.
201. H. C. Hang, J. Loureiro, E. Spooner, A. W. van der Velden, Y. M. Kim, A. M. Pollington, R. Maehr, M. N. Starnbach and H. L. Ploegh, *ACS Chem. Biol.*, 2006, **1**, 713-723.
202. K. Hanada, M. Tamai, M. Yamagishi, S. Ohmura, J. Sawada and I. Tanaka, *Agr. Biol. Chem. Tokyo*, 2014, **42**, 523-528.

203. D. Greenbaum, K. F. Medzihradzky, A. Burlingame and M. Bogyo, *Chem. Biol.*, 2000, **7**, 569-581.
204. N. Onda, S. Kemmochi, R. Morita, Y. Ishihara and M. Shibutani, *Transl. Oncol.*, 2013, **6**, 628-637.
205. C. H. Tung, *Biopolymers*, 2004, **76**, 391-403.
206. J. K. Mito, J. M. Ferrer, B. E. Brigman, C. L. Lee, R. D. Dodd, W. C. Eward, L. F. Marshall, K. C. Cuneo, J. E. Carter, S. Ramasunder, Y. Kim, W. D. Lee, L. G. Griffith, M. G. Bawendi and D. G. Kirsch, *Cancer*, 2012, **118**, 5320-5330.
207. W. C. Eward, J. K. Mito, C. A. Eward, J. E. Carter, J. M. Ferrer, D. G. Kirsch and B. E. Brigman, *Clin. Orthop. Relat. Res.*, 2013, **471**, 834-842.
208. P. Habibollahi, J. L. Figueiredo, P. Heidari, A. M. Dulak, Y. Imamura, A. J. Bass, S. Ogino, A. T. Chan and U. Mahmood, *Theranostics*, 2012, **2**, 227-234.
209. V. Ntziachristos, C. H. Tung, C. Bremer and R. Weissleder, *Nat Med*, 2002, **8**, 757-760.
210. A. A. Bogdanov, C. P. Lin, M. Simonova, L. Matuszewski and R. Weissleder, *Neoplasia*, 2002, **4**, 228-236.
211. C. Bremer, C. H. Tung, A. Bogdanov, Jr. and R. Weissleder, *Radiology*, 2002, **222**, 814-818.
212. U. Mahmood, C. H. Tung, Y. Tang and R. Weissleder, *Radiology*, 2002, **224**, 446-451.
213. E. Gounaris, C. H. Tung, C. Restaino, R. Maehr, R. Kohler, J. A. Joyce, H. L. Ploegh, T. A. Barrett, R. Weissleder and K. Khazaie, *PLoS One*, 2008, **3**, e2916.
214. E. Gounaris, J. Martin, Y. Ishihara, M. W. Khan, G. Lee, P. Sinh, E. Z. Chen, M. Angarone, R. Weissleder, K. Khazaie and T. A. Barrett, *Inflamm. Bowel Dis.*, 2013, **19**, 1339-1345.
215. M. Shrivastav, E. Gounaris, M. W. Khan, J. Ko, S. H. Ryu, M. Bogyo, A. Larson, T. A. Barret and D. J. Bentrem, *PLoS One*, 2018, **13**, e0206568.
216. M. P. Luciano, S. N. Croke, S. Nourian, I. Dingle, R. R. Nani, G. Kline, N. L. Patel, C. M. Robinson, S. Difilippantonio, J. D. Kalen, M. G. Finn and M. J. Schnermann, *ACS Chem. Biol.*, 2019, **14**, 934-940.
217. J. C. Widen, M. Tholen, J. J. Yim and M. Bogyo, *Methods Enzymol.*, 2020, **639**, 141-166.
218. R. J. Iwatate, M. Kamiya and Y. Urano, *Chemistry*, 2016, **22**, 1696-1703.
219. X. W. Ma, X. Li, S. L. Wang, J. Wang and Y. H. Wang, *J. of Nuc. Med.*, 2019, **60**.
220. E. Aikawa, M. Nahrendorf, D. Sosnovik, V. M. Lok, F. A. Jaffer, M. Aikawa and R. Weissleder, *Circulation*, 2007, **115**, 377-386.
221. M. Nahrendorf, P. Waterman, G. Thurber, K. Groves, M. Rajopadhye, P. Panizzi, B. Marinelli, E. Aikawa, M. J. Pittet, F. K. Swirski and R. Weissleder, *Arterioscler. Thromb. Vasc. Biol.*, 2009, **29**, 1444-1451.
222. M. Nahrendorf, D. E. Sosnovik, P. Waterman, F. K. Swirski, A. N. Pande, E. Aikawa, J. L. Figueiredo, M. J. Pittet and R. Weissleder, *Circ. Res.*, 2007, **100**, 1218-1225.
223. J. Chen, C. H. Tung, U. Mahmood, V. Ntziachristos, R. Gyurko, M. C. Fishman, P. L. Huang and R. Weissleder, *Circulation*, 2002, **105**, 2766-2771.
224. C. J. Goergen, H. H. Chen, A. Bogdanov, D. E. Sosnovik and A. T. Kumar, *J. Biomed. Opt.*, 2012, **17**, 056001.
225. F. Cattaruzza, V. Lyo, E. Jones, D. Pham, J. Hawkins, K. Kirkwood, E. Valdez-Morales, C. Ibeakanma, S. J. Vanner, M. Bogyo and N. W. Bunnett, *Gastroenterology*, 2011, **141**, 1864-1874 e1861-1863.
226. A. Wunder, C. H. Tung, U. Muller-Ladner, R. Weissleder and U. Mahmood, *Arthritis Rheum.*, 2004, **50**, 2459-2465.
227. V. Cortez-Retamozo, F. K. Swirski, P. Waterman, H. Yuan, J. L. Figueiredo, A. P. Newton, R. Upadhyay, C. Vinegoni, R. Kohler, J. Blois, A. Smith, M. Nahrendorf, L. Josephson, R. Weissleder and M. J. Pittet, *J. Clin. Invest.*, 2008, **118**, 4058-4066.
228. T. Christen, M. Nahrendorf, M. Wildgruber, F. K. Swirski, E. Aikawa, P. Waterman, K. Shimizu, R. Weissleder and P. Libby, *Circulation*, 2009, **119**, 1925-1932.
229. S. Ding, R. E. Blue, D. R. Morgan and P. K. Lund, *Inflamm. Bowel Dis.*, 2014, **20**, 363-377.
230. J. L. Cutter, N. T. Cohen, J. Wang, A. E. Sloan, A. R. Cohen, A. Panneerselvam, M. Schluchter, G. Blum, M. Bogyo and J. P. Babilion, *PLoS One*, 2012, **7**, e33060.
231. E. Walker, M. Mann, K. Honda, A. Vidimos, M. D. Schluchter, B. Straight, M. Bogyo, D. Popkin and J. P. Babilion, *J. Am. Acad. Dermatol.*, 2017, **76**, 209-216 e209.
232. K. Marten, C. Bremer, K. Khazaie, M. Sameni, B. Sloane, C. H. Tung and R. Weissleder, *Gastroenterology*, 2002, **122**, 406-414.
233. L. Josephson, U. Mahmood, P. Wunderbaldinger, Y. Tang and R. Weissleder, *Mol. Imaging*, 2003, **2**, 18-23.